Structural Optimization for Automated Fiber Placement

Andrew Atkinson

A thesis
submitted in partial fulfillment of the
requirements for the degree of

Master of Science

University of Washington

2022

Reading Committee:

Marco Salviato, Chair

Francesco Deleo

Program Authorized to Offer Degree:
Aeronautical & Astronautical Engineering

University of Washington

Abstract

Structural Optimization for Automated Fiber Placement

Andrew Atkinson

Chair of the Supervisory Committee:
Associate Professor Marco Salviato
Aeronautical Engineering

Structural optimization has long been used with isotropic materials to provide a preliminary design of components for revision toward a final part. Generative solutions closer to this final state can be obtained by implementing additional constraints in the optimization process. These constraints can be manufacturing, functional, or otherwise. For example, in a printed structure, a manufacturing constraint might limit the minimum member cross-section in the print plane. Implementing constraints for use with fiber-resin composite materials has been a more recent development, and an active area of research.

Fiber-composite laminates manufactured using the process of Automated Fiber Placement (AFP) have their own unique manufacturing requirements which existing commercial optimization suites do not adequately address. This results in "optimal" ply shapes which cannot be realized. This thesis describes and demonstrates a manufacturing constraint within an existing optimization process, such that the modified process results in plies which meet the minimum tow length constraint of AFP.

This novel constraint was then demonstrated on a test panel. Designed using T800/3900 carbon fiber prepreg, it features stress concentrations in the form of rounded corners and a 787-window cutout. The performance characteristics of the modified and current state-of-art panels were evaluated using finite element models. Finally, the modified ply boundaries were interpreted via AFP CAM software to validate their manufacturability.

This demonstration resulted in a panel that was 8g (1.6%) heavier than the standard optimization process with 1% increases to stiffness and strength. While still maintaining a 40% mass reduction over a comparable strength "black aluminum" panel. Crucially, this panel also has plies which can be accurately manufactured via AFP directly from the optimization output, as verified via CAM software. This makes the design process easier and faster.

TABLE OF CONTENTS

LIST OF FIGURES

LIST OF TABLES

GLOSSARY

AUTOMATED FIBER PLACEMENT (AFP): A process by which composite parts are manufactured using automation equipment.

HEAD: Common nomenclature for the AFP end effector, deposits material on the tool.

TOW: A single strip of composite material, stored on bobbins on the AFP machine, typically $\frac{1}{8}$ to $\frac{1}{2}$ inches wide.

COURSE: The tows deposited by an AFP machine in a single pass, without lifting the head off the layup tool.

PLY: Parallel courses laid next to each other to create a single layer of material with a specific fiber orientation.

LAMINATE: Many layers of material stacked and bonded together to create a single part.

PLYSTACK: The stack of material layers which describe a laminate. Commonly denoted with the notation [x°, y°, etc.], where x and y are the ply angles in the sequence.

CAM: Computer Aided Manufacturing, software which interprets a computer model into machine-readable M- and G- code, which directly drives a machine-tool via the CNC.

CNC: Computer Numerical Control, a process by which a part program is used to operate a machine tool. In contrast to manual operation, where an operator directly controls a machine's axes.

ACKNOWLEDGMENTS

Many thanks to University of Washington professors Marco Salviato, Jeff Wollschlager, and Francesco Deleo. Their instruction and guidance has been invaluable through this process.

Chapter 1

INTRODUCTION

1.1 Composites Manufacturing

Traditionally, composite laminates are made via the labor intensive "hand layup" process. As shown in Fig. 1.1, fabric sheets are pre-trimmed, and placed by hand onto a tool to build up a laminate's plystack. This laborious process can be expedited using assisting technologies such as laser projectors or other aids.

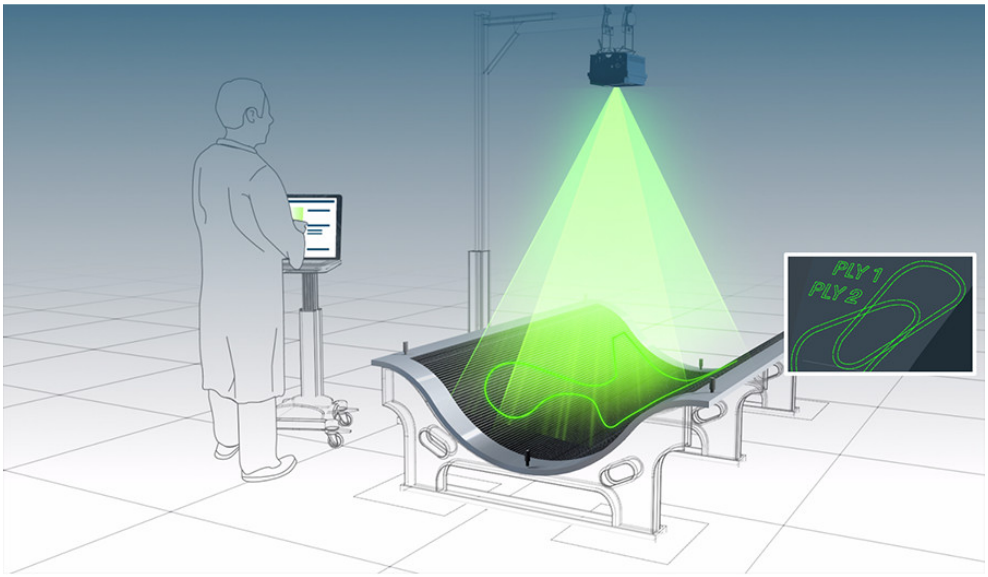

Figure 1.1: Ply boundaries projected onto a part for hand-layup. [1]

This method has some strengths compared to Automated Fiber Placement:

1. Lower Capital Costs: At their most basic, a plystack can be manufactured using nothing more than a skilled technician, a bolt of material, a knife, and the tool to drape the fabric over.

2. Woven Fabrics: Woven fabrics are easier to work with than unidirectional ones. Their interlaced fibers allow uncured material to be handled without damage, and different weaves can be used to tailor a desired material property. [2]

3. Design Flexibility: These woven fabrics are trimmed on flat cutting tables, so the ply edge geometry is not constrained by manufacturing limitations. These plies can then be formed by hand into tight corners, or other complex tool geometries without regard for machine constraints. [2]

As the scale of composite manufacturing has increased, technology has developed past simply assisting in hand layup techniques, more fully automating the manufacturing process. The current state of the art is automated fiber placement (AFP) as shown in Fig. 1.2. Here, spools of unidirectional ribbons of fiber, known as tows, are loaded on a machine. This machine then runs a program, similar to a CNC mill or other common machine tool, which uses the spools of raw material to build a plystack on the layup tool. This process can run with limited human intervention, though in practice almost 30% of total cell utilization time is dedicated to manual inspection of plies [3]. The dramatically increased initial capital investment required for an AFP cell is offset in part by the following advantages:

1. Reduced Labor Costs: An AFP cell requires only a fraction of the personnel to reach the same output of an equivalent manual production department. Additionally, the craftsmanship required to produce exceptional parts consistently is reduced.

2. Increased Part Envelope: Regardless of a technician's determination, due to the size of plies involved it is impractical to manufacture a 787 full-barrel fuselage section with hand layup methods. See Fig. 1.2.

3. Increased Repeatability: Once a program is proved, it will run consistently afterward, resulting in reduced variability between manufactured articles.

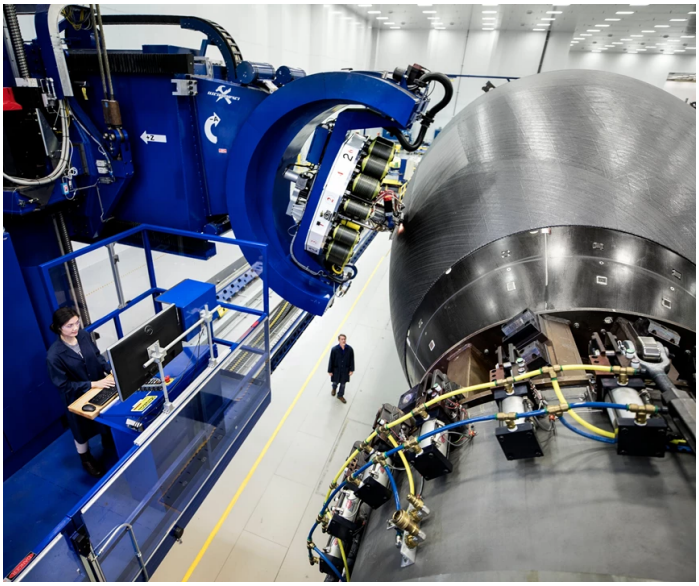

Figure 1.2: A 787's fuselage section #41 being manufactured, humans for scale. [4]

4. Improved Material Properties: Woven fabrics create deviations in material orientation as the fibers cross above and below each other. As a result, unidirectional tows have increased strength compared to woven fabrics [5]. These also reduce the material's longitudinal stiffness, as these crimps can be stretched out more easily. [2]

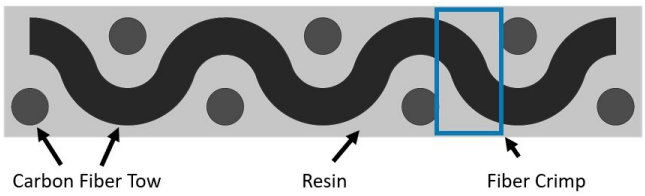

Figure 1.3: Stress concentration in a woven cloth's cross section. [2]

Reconciling the two manufacturing methods to take advantage of the strengths of both is an ongoing process. The mechanical and process advantages of AFP are desirable, but the restrictions on component geometry are a hindrance to designers. Creating tools which allow designers to easily create manufacturable parts is the goal of this research.

1.2 Structural Optimization

The field of structural optimization began over one hundred years ago with the work of A.G. Michell. In his paper "The limits of economy of material in frame-structures" [6], Michell demonstrated a method by which the Principle of Virtual Work can be used to minimize the elastic energy in a structure under a given load. This provides an example of the classical constrained structural optimization problem:

$$\begin{aligned} \text{Minimize:} \quad & \text{Strain Energy} \\ \text{Subject To:} \quad & \sigma_1 < \sigma_{yield} \\ & \sigma_2 < \sigma_{yield} \\ & \sigma_3 < \sigma_{yield} \\ & \vdots \\ & \sigma_n < \sigma_{yield} \end{aligned} \tag{1.1}$$

This syntax describes some objective function to be minimized, subject to a set of constraints. Here, the objective minimizes the total strain energy in a structure, while ensuring that no member's stress (σ_n) exceeds its yield stress (σ_{yield}). It is important to note that these are not the only objectives and constraints which may be designed around. Other examples include maximizing the first resonant frequency, minimizing manufacturing time [7], or minimizing mass. Further, these responses can also be used as *constraints* rather than objectives, e.g. minimize strain energy from a given loading condition, while constraining mass under a given value.

While Michell's work dealt with continuous structures and was relatively abstract, Prager built on this work 60 years later and discretized the problem [8]. In this classic example, a load 'Q' is being supported by anchors 'A' and 'B' using the members shown. Prager's work paved the way to use the finite element method for structural optimization problems in the coming decades. This, combined with the explosion of computing power available to the individual, meant that it was finally possible for the individual engineer to use structural optimization for component level part design.

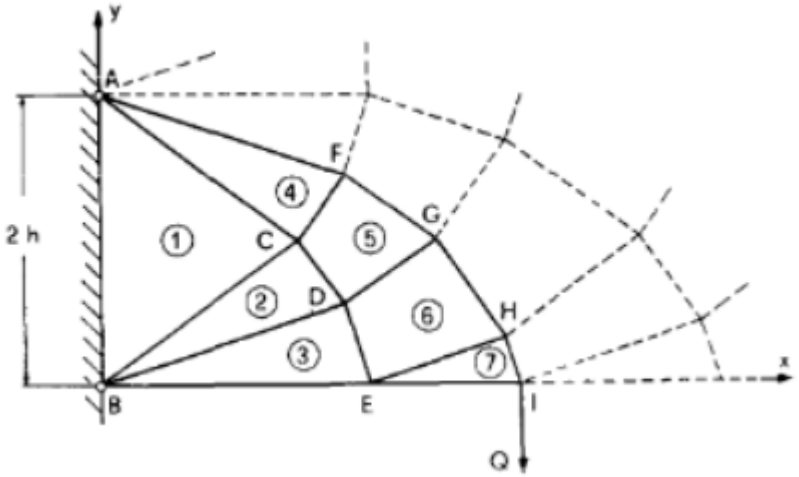

Figure 1.4: Example Prager Truss. [8]

Many groups have moved to capitalize on this new opportunity, resulting in multiple commercial products and even more private solutions. A few public options are Dassault Systems' "TOSCA" suite for use with Abaqus, Vrand's "Genesis", and Altair's "Optistruct". No comparison is made here between the features of these products.

1.3 Recent Composites Optimization Research

As mentioned in the abstract, the introduction of anisotropic materials to structural optimization has been a more recent phenomenon. Much of the current research in this area is regarding taking advantage of the new properties of fiber-resin composites within the optimization process.

This can take many forms. One example is the research by Esposito et al. with regard to tow steering the fibers of a laminate, in order to optimize the structure of a panel for a given loading condition. The results of this research are shown in Fig 1.5, and the research concluded by manufacturing the optimized panel on a Coriolis AFP machine. Similar research with regard to curvilinear fibers was conducted by Salviato et al. in "An Isogeometric Framework for the Modeling of Curvilinear Anisotropic Media" [9]. This field of work results in ply geometry which uses curved fibers to minimize stress in a part.

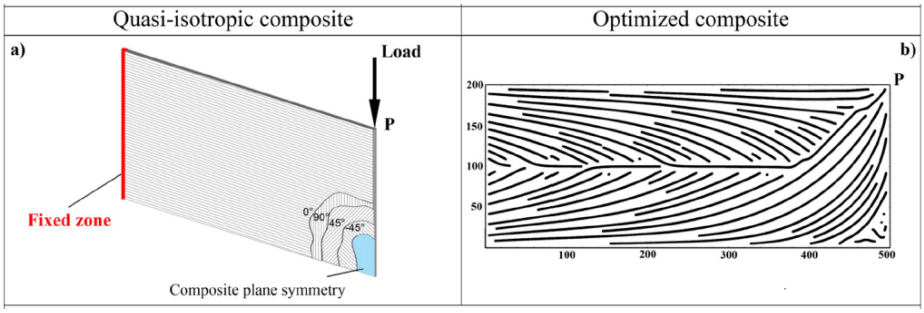

Figure 1.5: Curvilinear fibers optimized for a given loading condition [10]. Compare to the enhanced Optistruct results in Appendix A

Another example of research into composite optimization is in the area of manufacturing constraint implementaion. One example is Chuan Lo and James Guest's work in "Optimizing Topology and Fiber Orientations with Minimum Length Scale Control in Laminated Composites" [11]. There, they acknowledge the need for the application of a minimum length scale for composite ply optimization, and demonstrate a method by which this can be implemented, the result of which is shown in Fig 1.6.

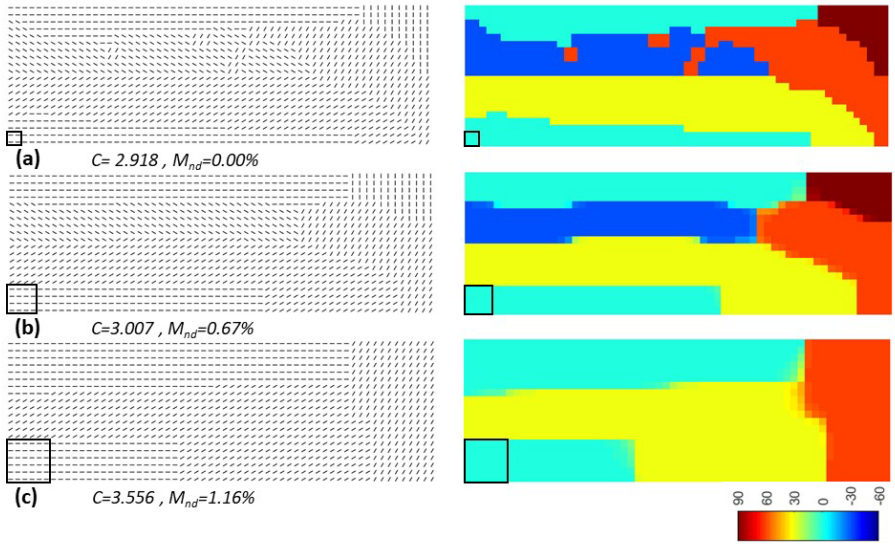

Figure 1.6: Minimum scale for a ply's geometry, as defined by a square region. [11]

The former papers demonstrate one of the value-add capabilities of AFP in the form of tow-steering, and the latter solves a necessary problem with optimization in its pursuit of manufacturability. However, neither directly targets the minimum tow length constraint unique to the AFP process, described in section 2.3 and illustrated in Fig 2.7 .

Chapter 2

MODERN OPTIMIZATION SOFTWARE

Today, commercial solutions are available to satisfy an engineer's needs for general purpose optimization problems. Due to its integrated composites functionality, Altair's Optistruct was selected for use in this study. Optistruct was released in 1994, and its first commercial customer was General Motors for use in automotive design. [12]

2.1 Problem Definition

Prior analysis yields the component profile to be further refined via structural optimization e.g. a fuselage or aircraft wing's shape is defined by requirements other than structural performance, for example aerodynamics. In this case, the geometry selected is representative of a section of an aircraft's fuselage. This small section was chosen for its compatibility with lab-based tensile testing equipment, and stress concentrations which create interesting ply profiles. This geometry is then imported to Optistruct for analysis.

Once loaded, a finite element mesh is created. Material properties and boundary conditions are also defined here. For the remainder of this thesis the boundary conditions and properties in Fig. 2.1 and Table 2.1 will be considered for optimization. Additional boundary conditions are demonstrated in the appendices. The left edge is fully fixed, with all nodes constrained in six degrees of freedom. The right edge has all nodes constrained in five degrees of freedom, with the x-axis remaining free. All nodes on the right end are constrained to move equally in the x-axis. These boundary constraints simulate the clamping constraints of a tensile testing apparatus. A load of 100kN is applied to the right edge of the plate.

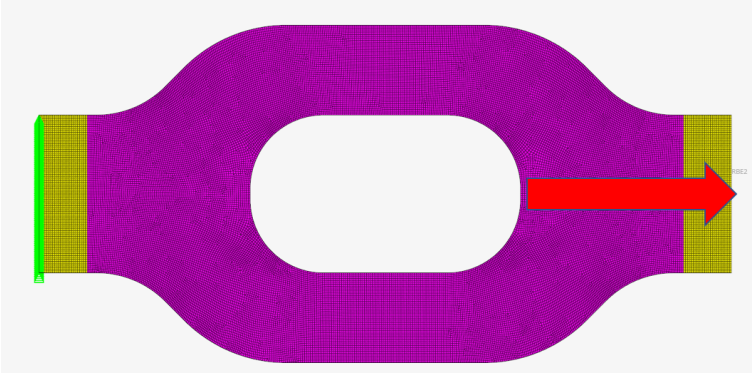

Figure 2.1: Boundary constraints of optimization demonstration panel.

E_1	E_2	ν_{12}	G_{12}	X_T	X_C	Y_T	Y_C	S	t
153GPa	8GPa	0.34	4GPa	2.8GPa	1.9GPa	56MPa	307MPa	90MPa	$\frac{1}{8}$mm

Table 2.1: CFRP material properties.

Prior to optimization, the design space is also defined. Fig. 2.2 illustrates this, showing the mesh with thicknesses of each element correlated to the ply profile associated with it. Each element contains 2mm of 0°, 90°, and ±45° plies, and the laminate is symmetric. This constrains the design space such that the final panel will be comprised of only 0°, 90°, and ±45° plies, with no more than 2mm of any one orientation in a given element.

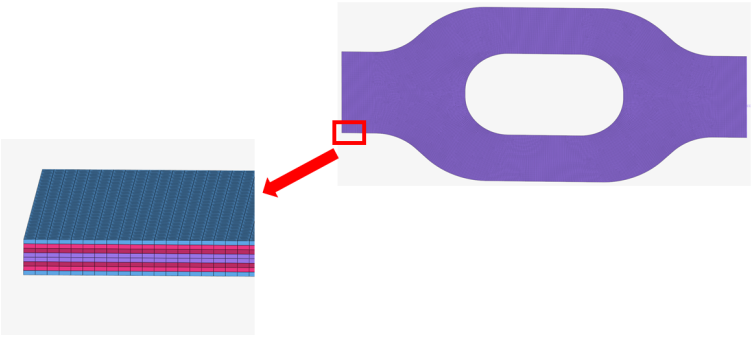

Figure 2.2: FE mesh and maximum material condition defined.

2.2 Optimization Process

Optistruct uses what its developers designate the "three phase optimization process" [13] for its composite optimization algorithm. These phases are as follows:

1. Free Size Optimization

   The optimization problem in its most general sense is defined and solved, yielding a "most ideal" result. In this case, the objective is to create the lightest panel, that can still withstand a specified loading condition as evaluated via Tsai-Wu failure criteria. Additionally, laminate thickness constraints are applied to prevent degenerate solutions. Equation 2.1 describes this constrained optimization problem:

$$\begin{aligned} \text{Minimize:} \quad & \text{Mass} \\ \text{Subject To:} \quad & \text{Failure Criteria} < 1 \\ & \text{Minimum \& Maximum Laminate Thickness} \\ & \text{Balanced \& Symmetric Laminate} \end{aligned} \tag{2.1}$$

   Where before every element had an equal quantity of each ply orientation, now the thicknesses of each orientation varies on an element-by-element basis. In Fig. 2.3 the thick 0° plies (now pink) are still present in the middle of the laminate, but other orientations are thinned. Note that these ply thicknesses are not specified as integer multiples of a specific thickness, and so are not manufacturable since fractional ply thicknesses are not possible.

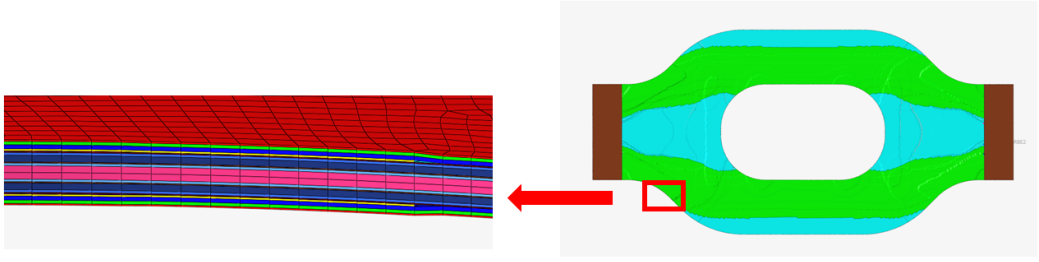

Figure 2.3: Plies resulting from free size optimization.

2. Composite Size Optimization

The free size result serves as a starting point for the application of additional constraints on the optimization. Now, the constraint that each ply must be equal to the actual material thickness is applied. This is constrained optimization problem can be written as follows:

$$\begin{aligned} \text{Minimize:} \quad & \text{Mass} \\ \text{Subject To:} \quad & \text{Failure Criteria} < 1 \\ & \text{Minimum \& Maximum Laminate Thickness} \\ & \text{Balanced \& Symmetric Laminate} \\ & \text{Ply Thickness} = \text{Specified Value} \end{aligned} \tag{2.2}$$

For example, if after the free size optimization a given region of a laminate contained a ply 0.340mm thick, following the composite size optimization this may be converted into three 0.125mm plies. This is not simply rounding; an iterative optimization is run to determine the new thicknesses, with the full suite of design constraints available. In principle, the initial free size step is not required, but better results are typically seen when starting with the free size optimization. [14]

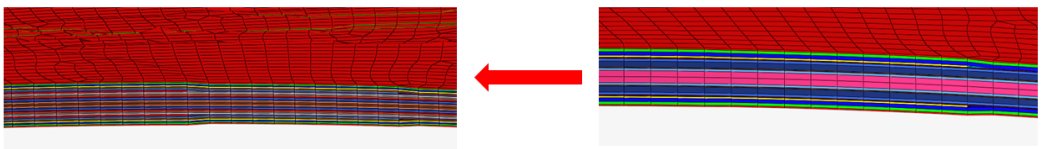

Figure 2.4: Plies resulting from composite size optimization.

3. Composite Ply Shuffling

Finally, the plies resulting from the composite optimization process are shuffled according to rules set by the designer. Examples of these rules include: -45°and 45° plies are consecutive, restrictions on consecutive plies in the same orientation, or certain plies on the outside of the laminate. Additionally, further optimization problems can be solved here, for example minimizing bending compliance to a secondary loading condition.

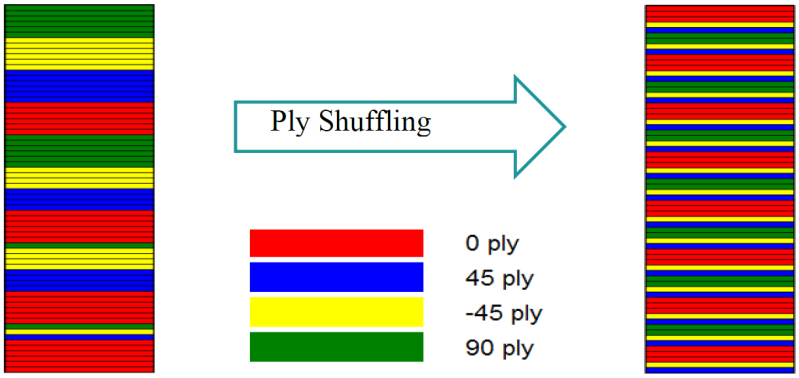

Figure 2.5: A plystack before and after shuffling. [14]

While this optimization sequence is undoubtedly useful, there is still room for improvement. While some manufacturing constraints are accounted for such as ply thicknesses, or maximum/minimum final laminate thickness, there are still additional constraints which can be added. One such constraint is the minimum tow length required by AFP. Implementing this reduces discrepancies between the optimization process's output, and a manufacturable final part.

2.3 Explanation of Minimum Tow Length Constraint

Currently using Optistruct, the minimum length-scale of the ply shapes' contours can be controlled by the solver, resulting in either very fine, granular, structures, or more gently rounded ones.

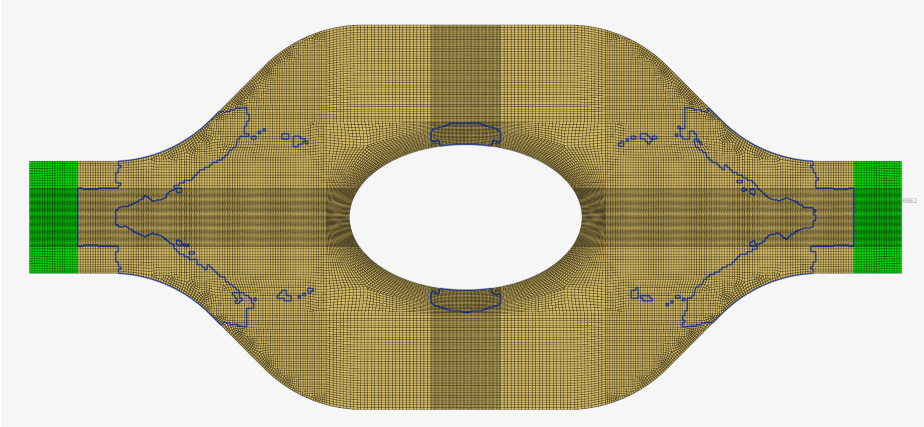

(a) No Minimum Length Scale

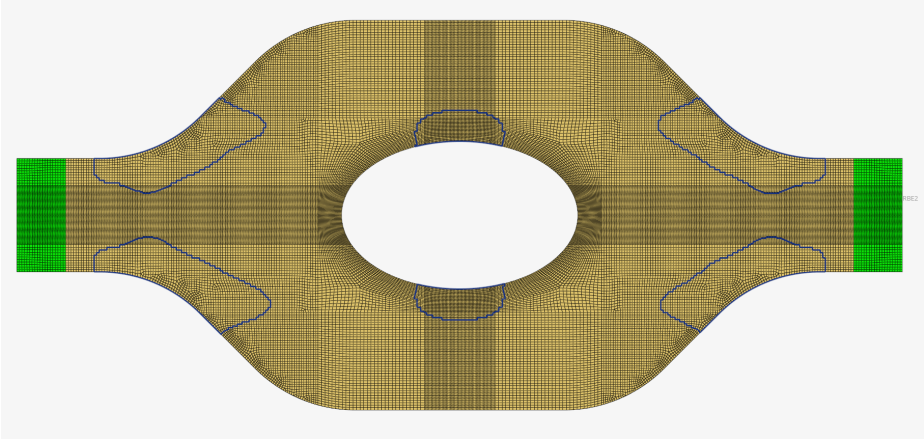

(b) 50mm Minimum Length Scale

Figure 2.6: Effect of a minimum length scale on ply's profile.

However this length scale constraint alone does not meet the minimum tow length requirement, as portions of the ply geometry will still violate the minimum length constraint of the AFP system.

AFP heads lay tows using a compaction roller to apply force between the material and tool, bonding the tows to the warmed tool or previously deposited plies. The minimum tow length is the distance from this knit point to the internal cutter module of the head, shown in red in Fig. 2.7. If a sub-minimum length tow were attempted, the tow would have no constraint on its placement, resulting in layup defects or machine issues.

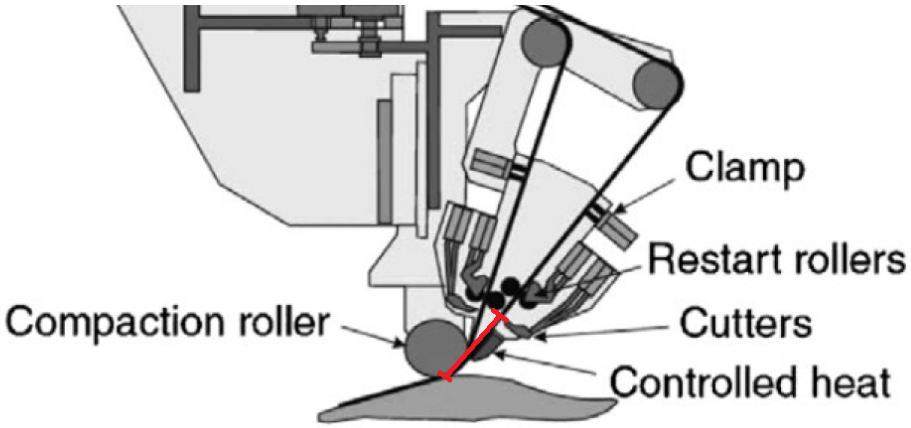

Figure 2.7: AFP head illustration, minimum length indicated in red. [15]

2.4 Altair's Implementation

Altair has actually attempted to solve this problem within the current release of Optistruct. However, the current approach has some problems, as described in the following. Fig. 2.8 shows the dialog for applying this constraint as currently implemented. Parameters defining the tows' widths and minimum lengths can be defined. Fig. 2.9 shows a 90° (vertical) ply designed using this constraint.

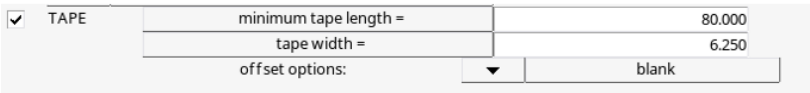

Figure 2.8: Optistruct's minimum tow constraint interface.

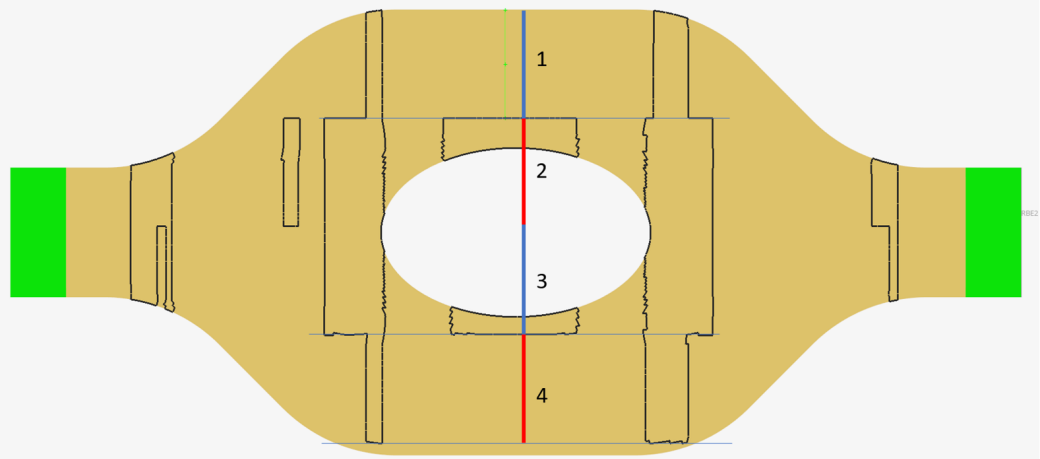

Figure 2.9: The result of Altair's minimum tow length constraint optimization.

This has multiple unexpected design features:

1. The ply boundaries are constrained as integer multiples of the minimum tow length. There are just over four minimum tow lengths to the bottom. These coincide with the tows' add and drop locations.

2. Not only are the tows' lengths constrained to multiples of the minimum, but their positions are also defined relative to the edge of the panel. Starting from the top of the panel, tows are added or dropped moving downward.

3. While the plate and loading condition has two lines of symmetry, the ply as designed has none. It would be expected, though not guaranteed, that some symmetry would be present in the finished ply given the load and boundary conditions. This is present in the non-constrained versions of the design problem, see Fig. 2.6.

While this approach does satisfy the minimum tow length requirement, it does so by *vastly* overconstraining the problem. An AFP machine can lay up a tow any length over the minimum, not strictly multiples of this length. Additionally, there is no reason a tow must start at the same point as its neighbors, or any particular point on the design space.

2.4.1 What is the current process doing?

When Altair's minimum tow constraint is active, the solver groups mesh elements into "meta-elements" the size of the minimum tow specified. These meta-elements start at the minimum X and Y mesh coordinates and cover the design space. For the remainder of the optimization process, the solver will modify ply geometry only on the scale of these meta-elements, rather than individual mesh elements. These meta-elements are not refreshed during the optimization process, and are not generated with regard to symmetries or other design considerations.

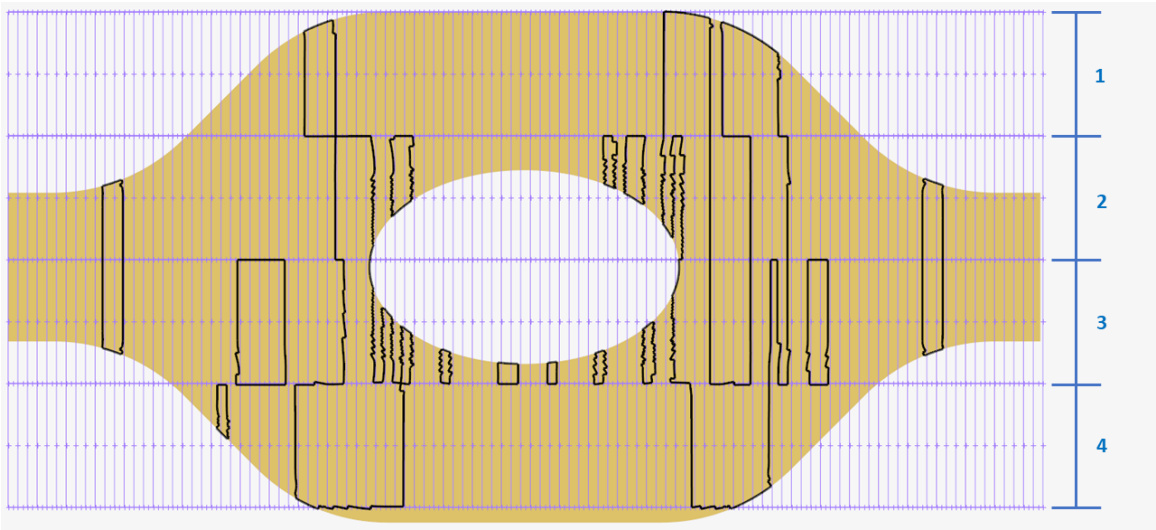

Figure 2.10: Illustration of meta-element boundaries as purple rectangles.

Chapter 3

NOVEL MINIMUM TOW-LENGTH CONSTRAINT IMPLEMENTATION

As described in Chapter 2, the current implementation of the minimum tow length constraint does not properly accommodate the requirements of AFP. As such, a novel constraint implementation must be developed in a robust and helpful manner. The new implementation adds an additional stage to the optimization process after composite optimization applying the following optimization problem:

$$\begin{aligned} \text{Minimize:} \quad & \text{Changes to Plies} \\ \text{Subject To:} \quad & \text{Failure Criteria} < 1 \\ & \text{Min-Tow Constraints} \end{aligned} \tag{3.1}$$

Which is to say: modify the sets of elements comprising the "true optimal" plies as little as possible, while maintaining the no-failure condition from before, and now applying the minimum tow constraint.

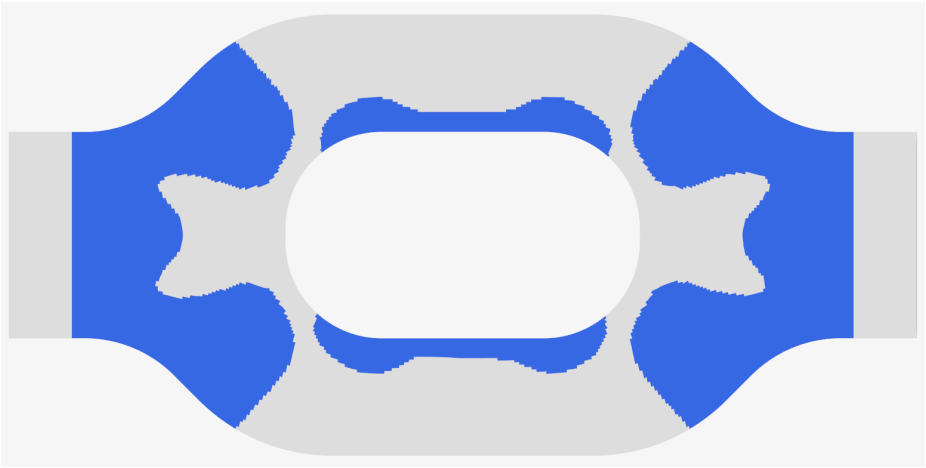

Figure 3.1: Example ply region in blue, as currently output from Optistruct.

3.1 Description of Methodology

In implementing this, the following operations are applied to each ply, after the current composite optimization step (step 2 from section 2.2) is carried out:

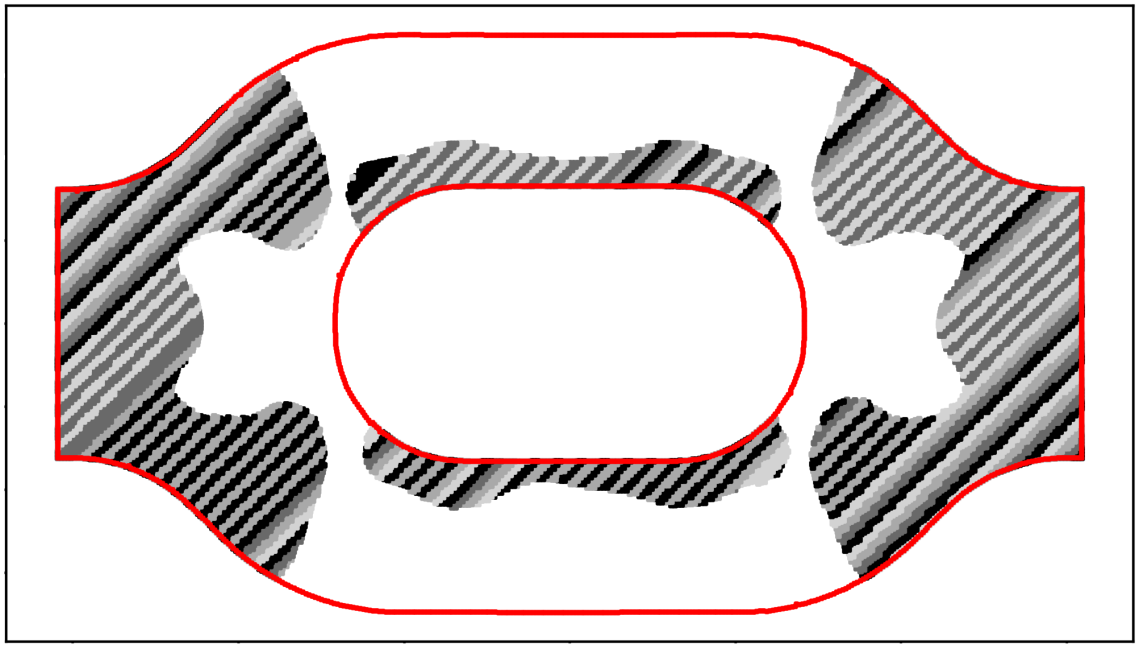

Figure 3.2: Example ply divided into 6mm wide tows.

First, the elements comprising each ply are parsed into strips with width equal to the tows used in the particular AFP machine. Fig 3.2 illustrates the result of this process. Care should be taken to group only contiguous elements together, as elements of the same strip may be separated by ply geometry. These separate regions are then required to be laid as separate tows, each with their own minimum length requirement.

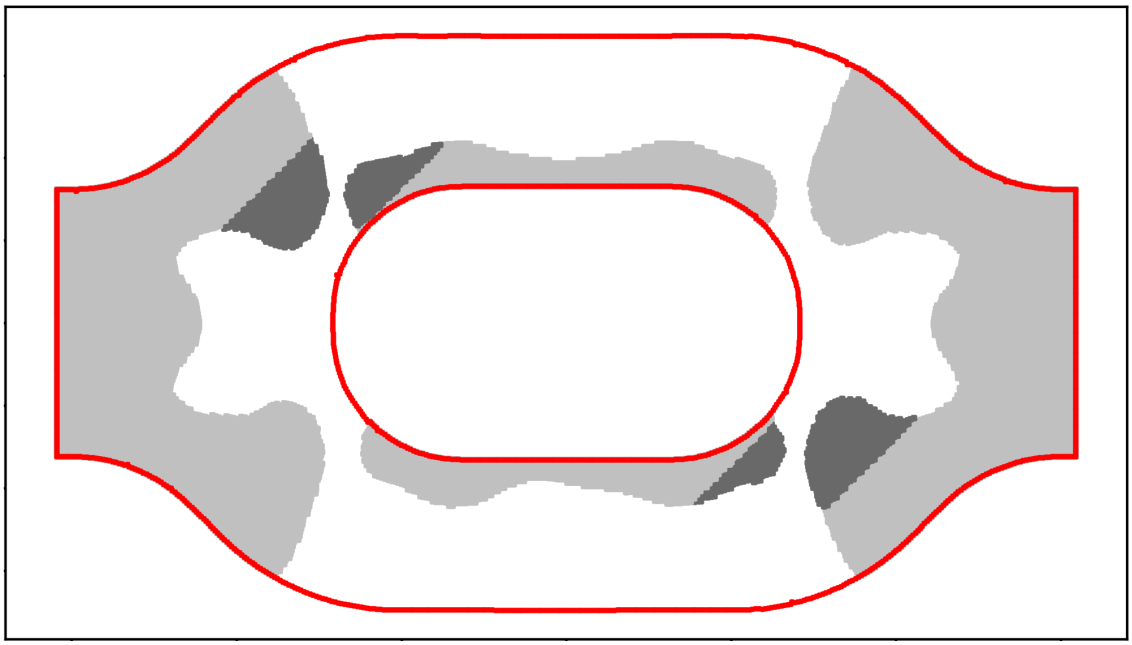

Figure 3.3: Tows which fail all manufacturing requirements indicated in dark grey.

Then, the length of each strip is evaluated, and problem strips are identified. Fig. 3.3 shows the results of this identification process. The full panel's perimeter is shown in red, the ply area suitable for AFP is shown in light gray, and areas in need of adjustment are highlighted in dark gray. It is important to note that factors besides minimum length must be considered for manufacturability. For example, if a sub-minimum tow contacts the panel's edge, the excess length may be placed outside the work area, and so the short tow is acceptable. This is most clearly demonstrated in the areas directly above and below the central window cutout.

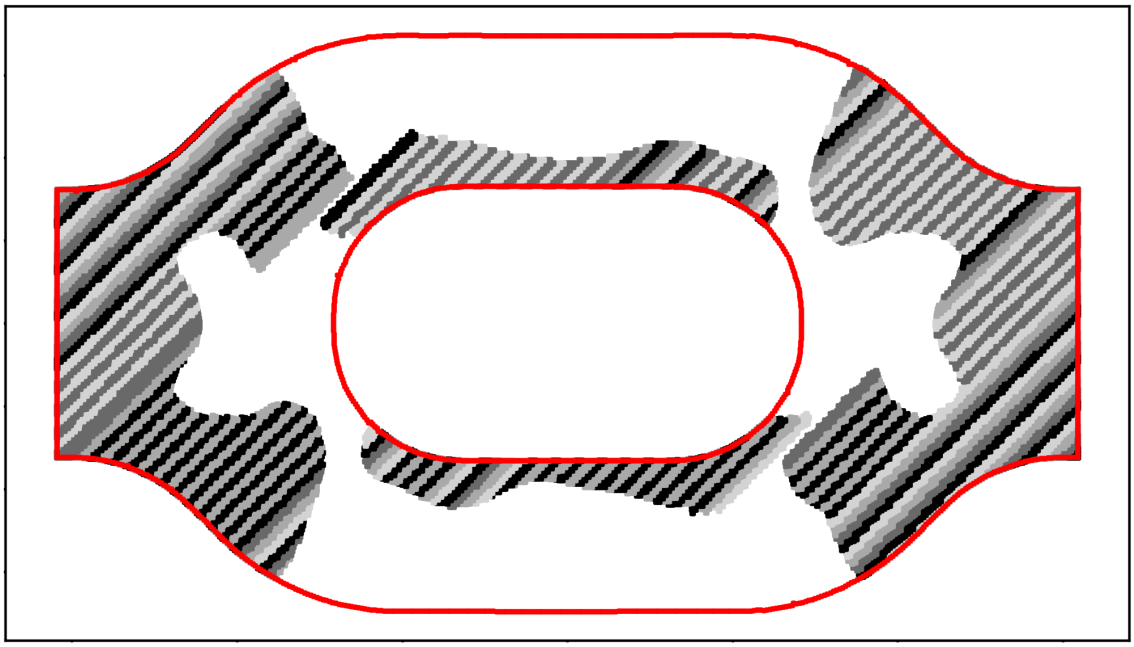

Figure 3.4: Problematic tows are adjusted, resulting in final ply geometry.

Finally, the problematic tows are either eliminated or elongated. Elongation is accomplished by adding elements on either side of the short tow, until the minimum tow length is reached. If this tow extension process causes the tow to contact the panel's edge, only the elements required to reach that edge are added to the tow, as the remainder can then be placed off the panel's boundary. The same will occur if the extended tow now contacts another region of the same ply, as they could now be laid up continuously as a single tow. The choice between elongation or elimination depends on the tow's initial length. For example, a tow which only contains one or two elements can often be eliminated entirely, whereas a tow which is only a millimeter short of the minimum length should usually be extended. The optimal value for this threshold requires iteration to evaluate.

Chapter 4

RESULT AND ANALYSIS

Following the addition of this step to the optimization process, a demonstration panel is designed and its performance evaluated. First, the structure of the panel is shown, illustrating the changes the minimum tow constraint generates. Then, the modified panel is contrasted with the output of the current optimization process. Finally, the modified panel's structural characteristics are evaluated, to ensure performance is not compromised.

4.1 Illustrations before and after AFP compatibility

A sample ply from the final laminate design is shown in Fig. 4.1. The corrected ply for an 80mm minimum tow length is shown as elements with a grey outline, and the original ply output is overlaid in yellow. The full plystack is shown in Fig. 4.3, further illustrating how the minimum tow length constraint modifies the ply profiles.

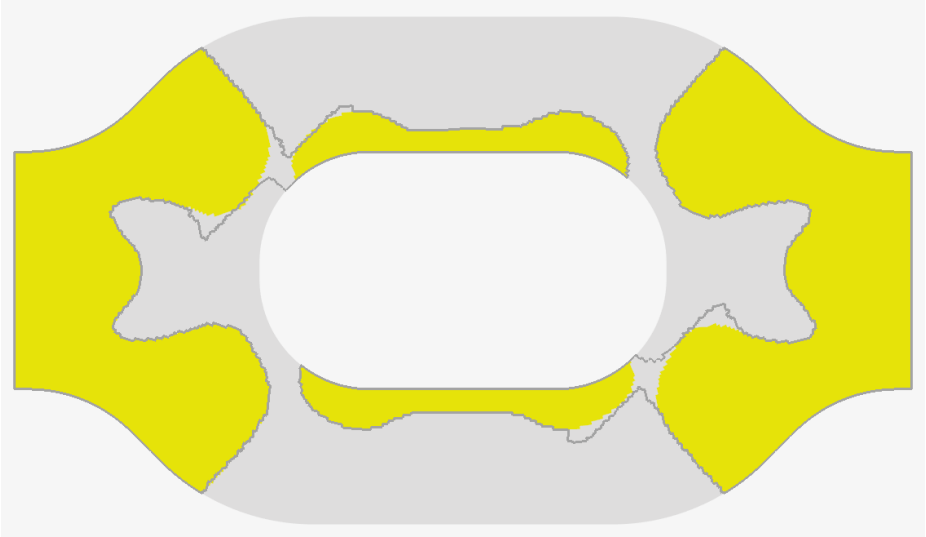

Figure 4.1: Example ply shown with and without the tow length constraint.

Note now that a ply which once had two axes of symmetry, now has a single 180° rotational symmetry. Additionally, where once -45° and 45° plies were constrained as identical, resulting in a balanced laminate, they will now commonly result in mirror images of each other as shown in Fig. 4.2. In principle, this minor imbalance may produce shear-extension coupling or other undesirable properties. In Classical Lamination Theory (CLT) this would be predicted by nonzero A_{16}, A_{26}, D_{16}, and D_{26} terms in the laminate's ABD matrix, and indeed, these are locally nonzero in these regions. However modelling the full panel does not display any measurable effects of this imbalance due to the extremely small areas concerned when compared to the overall panel's size.

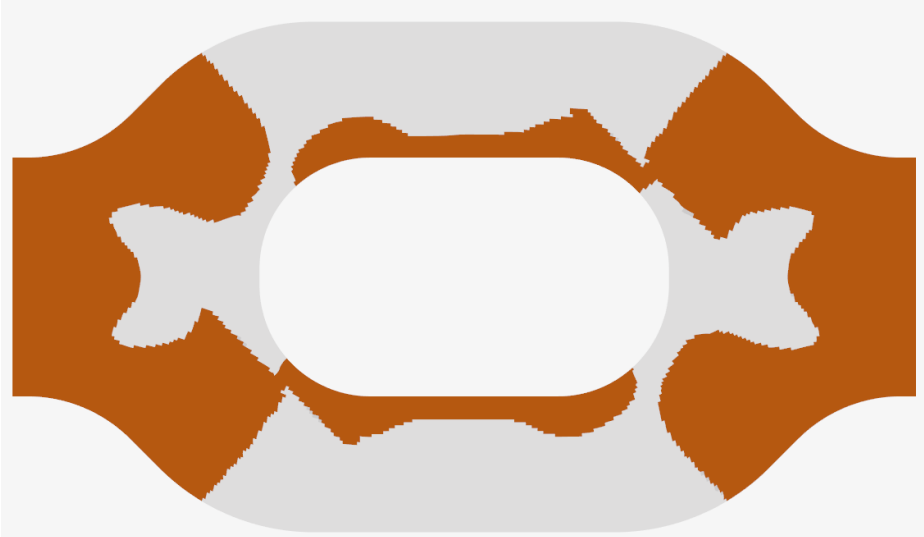

Figure 4.2: "Mirrored" counterpart -45° ply to the example ply in Fig. 4.1.

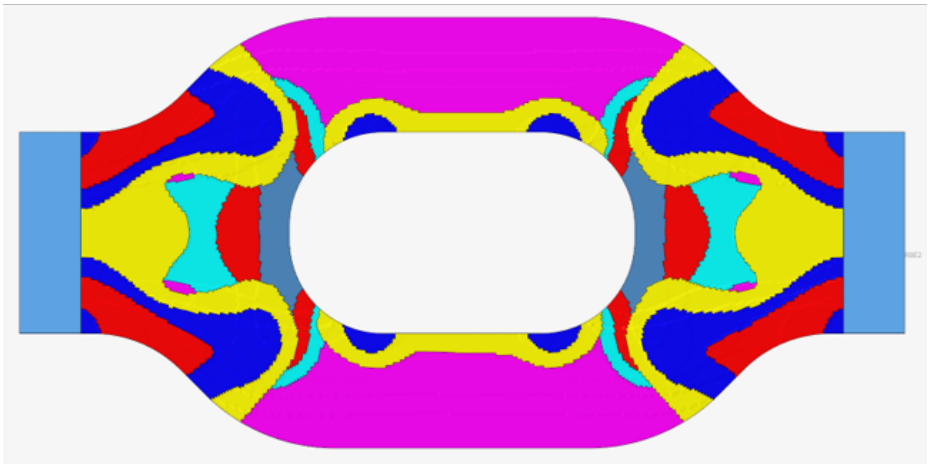

(a) Optimization result from current method.

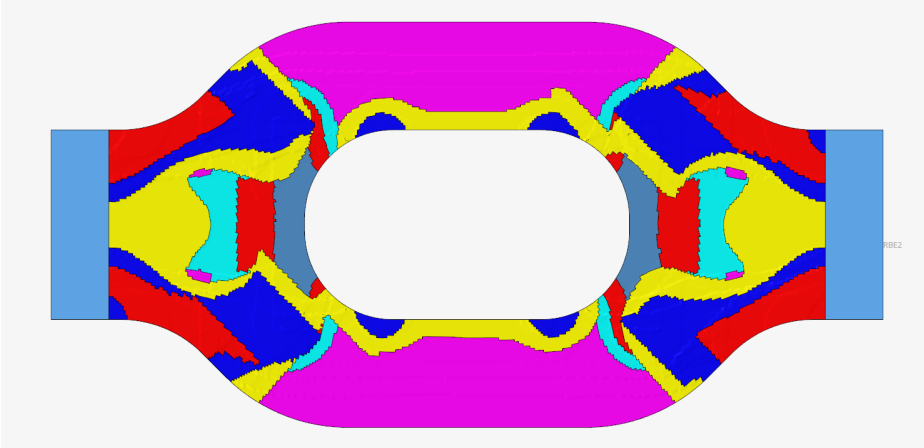

(b) Optimization result with minimum tow length constraint applied.

Figure 4.3: Demonstration panel's full plystack, before and after minimum tow constraint.

4.2 Structural Description

The fully recompiled plystack results in 121 distinct stacking sequences spread over the panel's area as shown in Fig. 4.4. The panel's overall thickness is shown in Fig. 4.5. The thinnest regions with only 4 plies are shown in blue, and the thickest in red with the maximum 36 plies. This complete laminate is now analyzed for structural properties.

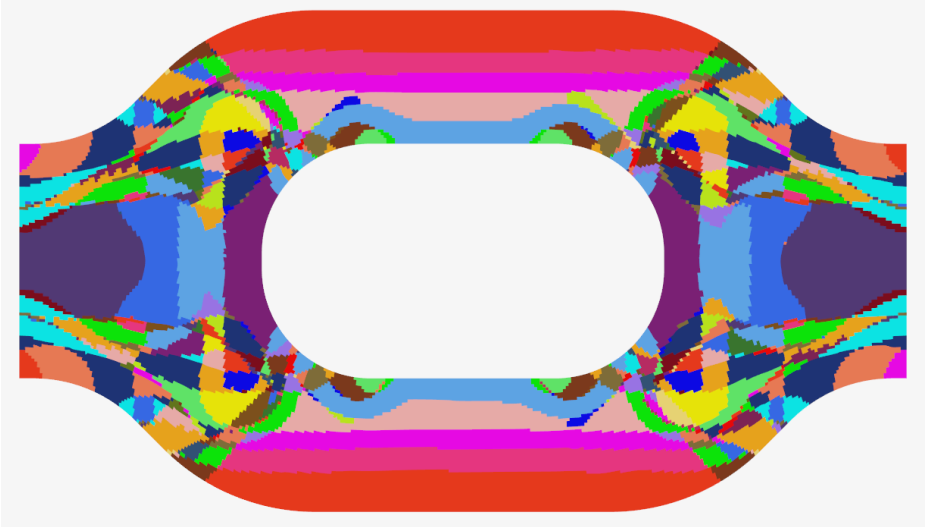

Figure 4.4: All 121 unique plystacks color-coded per element.

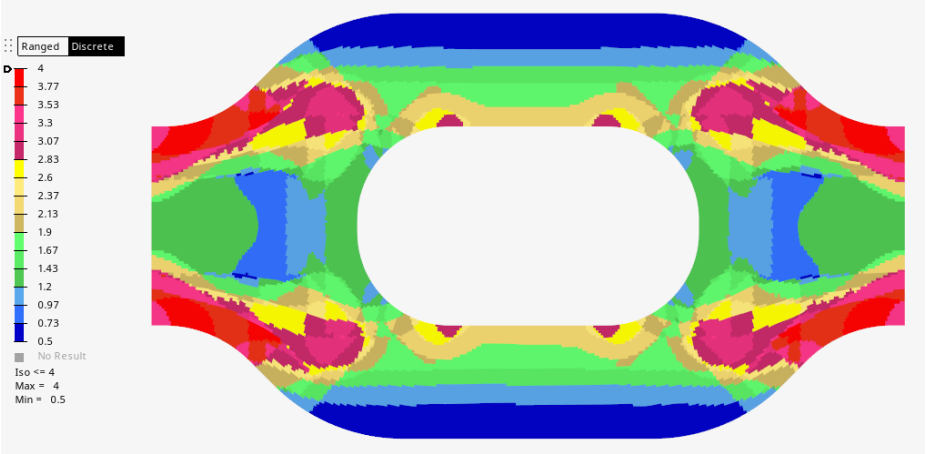

Figure 4.5: Panel thickness color-coded per element. (mm)

The effect of constraining the plies for minimum tow criteria is minimal. Total mass increased 1.6% from 0.495kg to 0.503kg, peak Tsai-Wu failure criteria lowered from 0.891 to 0.882, and maximum displacement lowered from 2.93mm to 2.89mm. However these increases in strength and stiffness represent efficiency loses, as the plate already met the design specifications, and mass has increased.

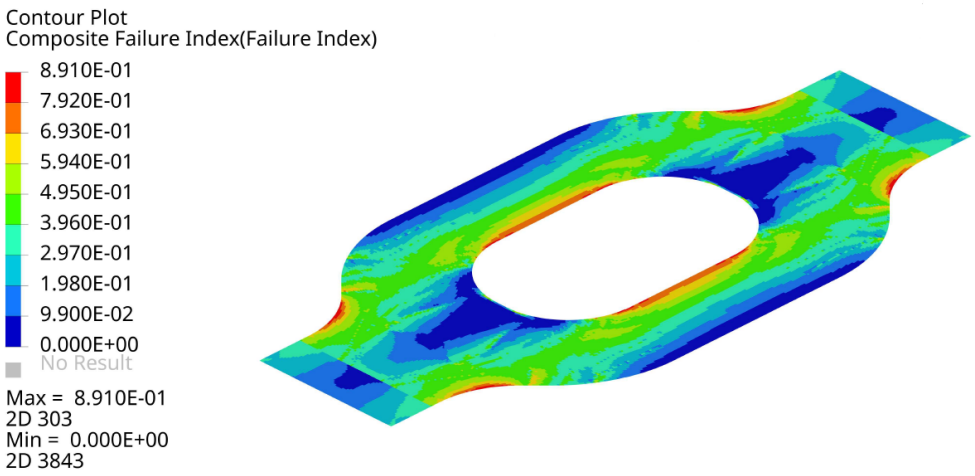

(a) Without the minimum tow length constraint.

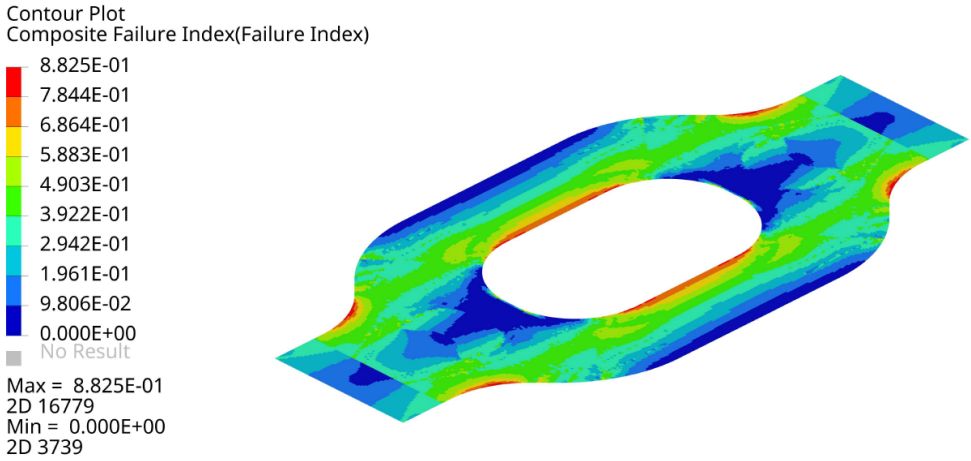

(b) With the minimum tow length constraint.

Figure 4.6: Contour plots of Tsai-Wu criteria with and without the tow length constraint.

4.3 Benefits of Optimization

It is worth evaluating the benefit optimization as a whole has in the design process. The clearest contrast is made by comparing the optimized ply structure to a naive solution of equal portions [0°, 90°, 45°, -45°] full-coverage plies, with equal mass between both laminates.

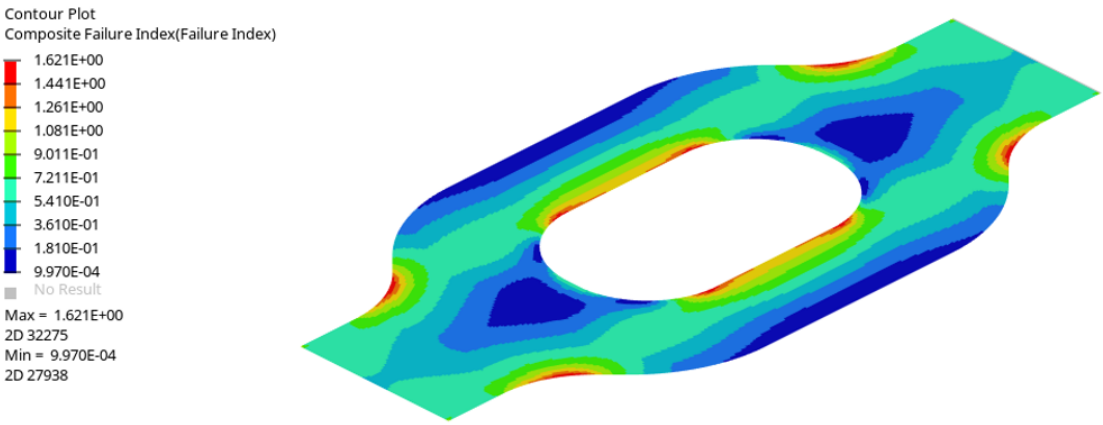

Figure 4.7: Contour plot of Tsai-Wu index with full coverage plies in equal proportions.

As the peak Tsai-Wu failure index is greater than 1, Fig. 4.7 indicates the "black aluminum" panel with equal mass to the optimized panel (0.503kg) would fail from the specified 100kN load. In fact, further testing shows that the panel would require a mass of 0.70kg to withstand the load. This represents a 40% mass efficiency gain from the optimization process.

4.4 Further Finite Element Analysis

Further simulations are carried out in Dassault's "Abaqus" finite element suite. Following the conversion from Hyperworks to Abaqus, an initial check is made to ensure everything is acting as it should.

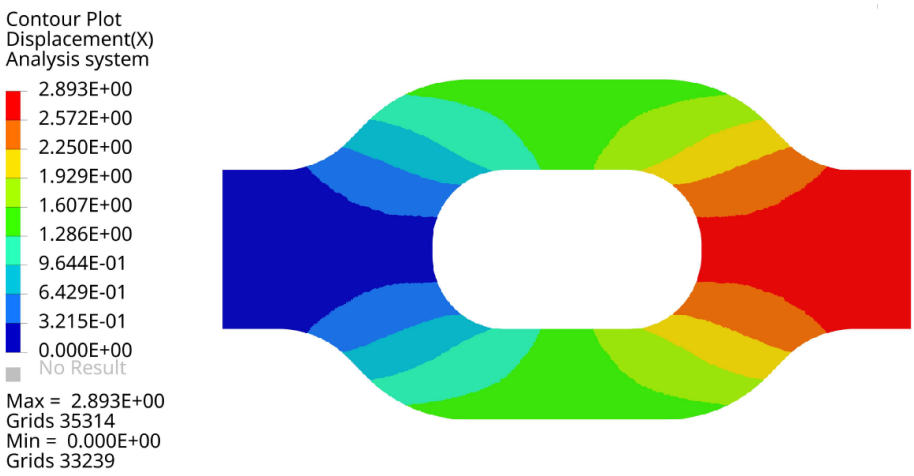

(a) 1-direction displacement plot in Hyperworks.

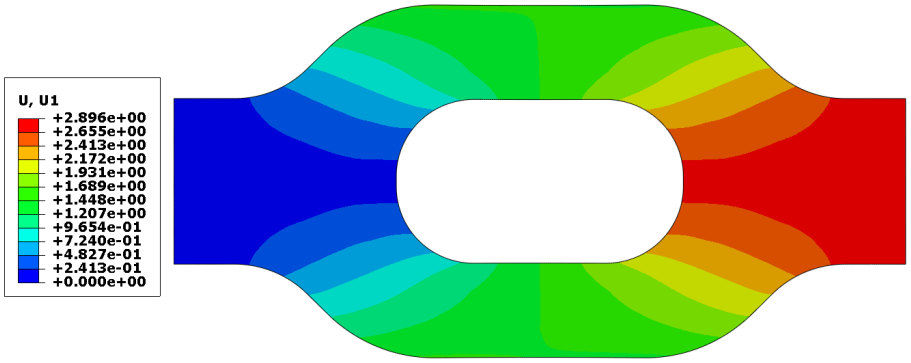

(b) 1-direction displacement plot in Abaqus.

Figure 4.8: Comparison of displacement predictions from Hyperworks to Abaqus. (mm)

Fig. 4.8 shows the peak displacements are within a couple microns of each other for the same boundary conditions, so the conversion is a success. Further analysis can be carried out in Abaqus with confidence. Running a dynamic simulation in Abaqus allows an analysis of damage propagation and more in-depth failure modeling. This analysis shows that the initial failure of the panel will occur in a buckling mode around the cutout. This occurs before material failure, but is in line with the buckling of composites featuring stress concentrations, as described by Kremer in [16].

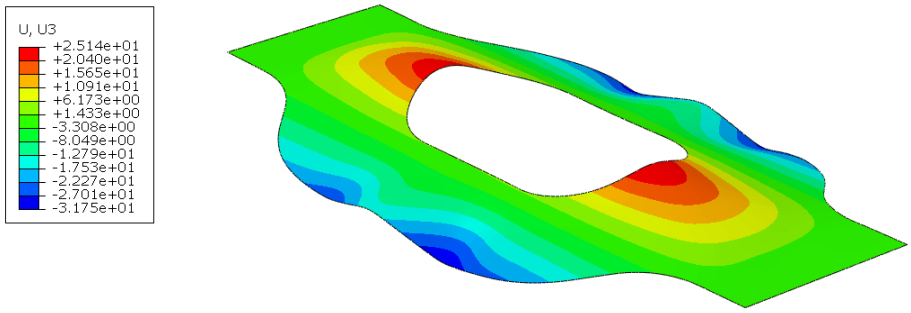

(a) Contour plot of out-of-plane displacement as computed via FEM.

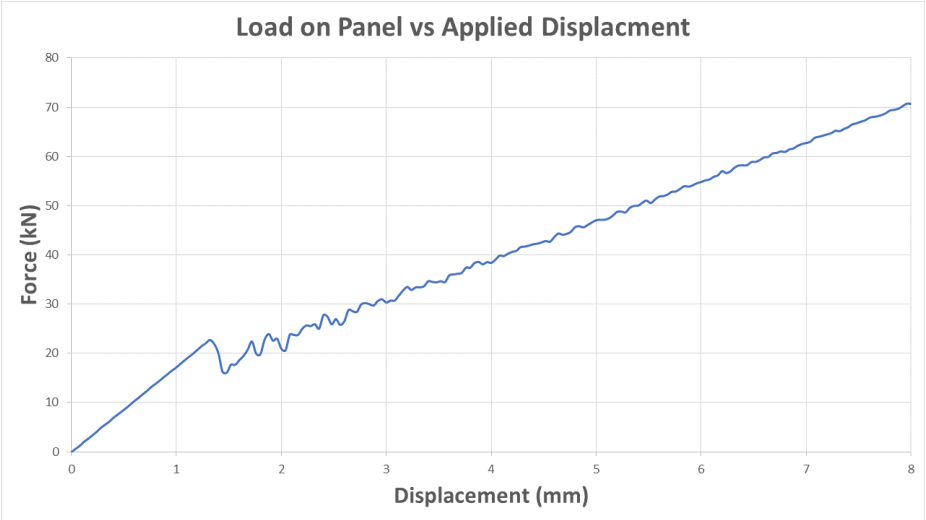

(b) Evolution of the reaction force as a function of applied displacement.

Figure 4.9: Illustration of tension induced buckling.

This failure mode has additional experimental evidence. When Aoki et al. [15] were creating their panel, they encountered the same issue and needed to add structural reinforcement to measure the desired failure modes. This failure mode is extremely difficult to accommodate through optimization, due to the nonlinear nature of buckling failures. This presents an opportunity to further refine the optimization process, but implementing this is beyond the scope of this thesis.

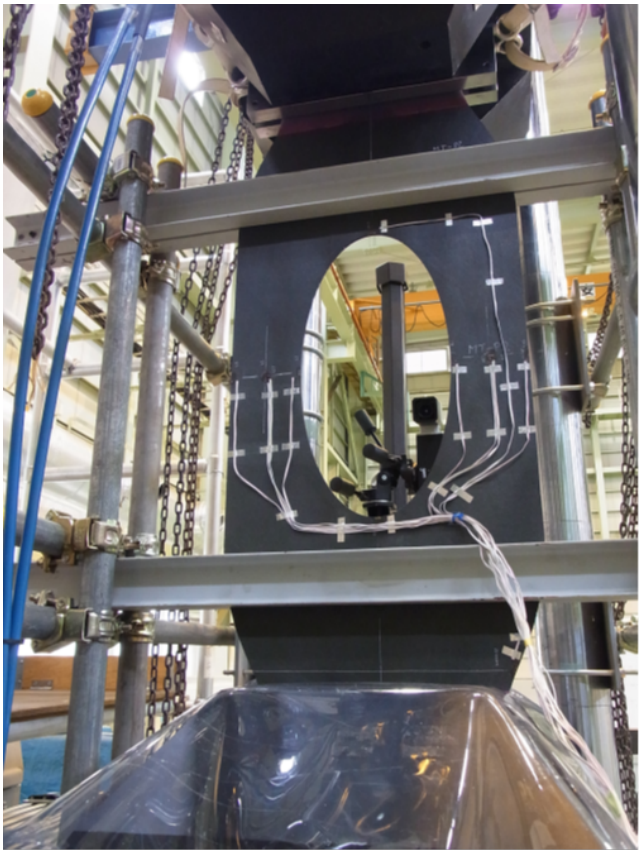

Figure 4.10: Metal reinforcement to bypass buckling failure during tensile testing. [15]

Suppressing the buckling mode by restricting nodal travel out of plane allows further analysis of crack propagation and ultimate failure mode. The first failure mode is a tensile failure in the matrix of the composite. This occurs as 3.5mm end displacement is applied, corresponding to a load of 121kN as shown in Fig. 4.11.

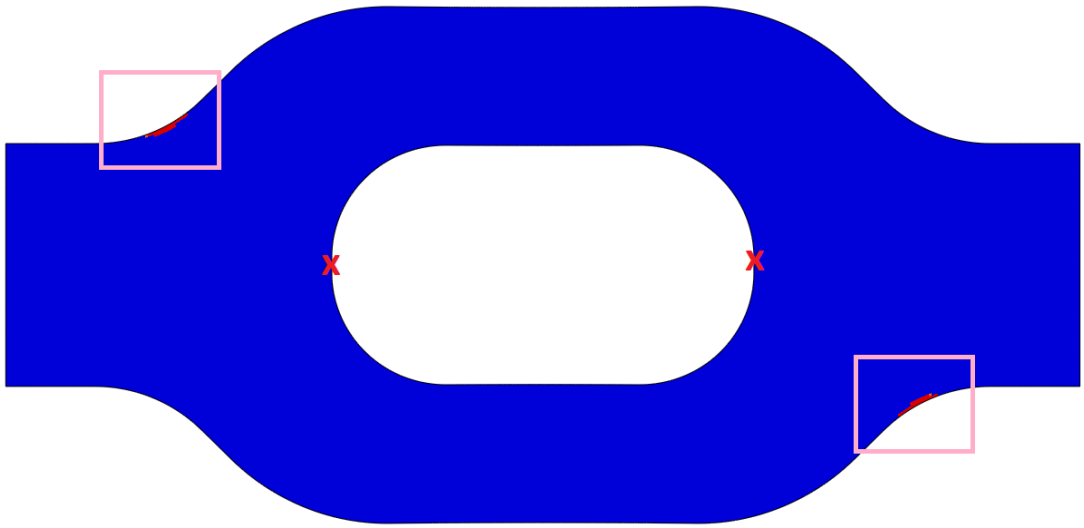

Figure 4.11: Red elements indicating tensile failure of the matrix.

However, even as the matrix failure region continues to spread, this has minimal effect on the stiffness of the panel, as illustrated in Fig. 4.12. The ultimate failure mode occurs from compression loading of fibers bordering the panel cutout. Once this failure occurs, the crack quickly propagates from the red 'X' initiation sites toward both ends of the plate, resulting in total structural failure. See Fig. 4.13.

Of note here is the ultimate tensile strength demonstrated by the panel relative to both the initial design specification as well as the analysis performed using Tsai-Wu failure criteria. Whereas the design specification calls for a minimum strength of 100kN, the strength predicted by the Tsai-Wu evaluation is 112kN. This design margin is primarily due to the inefficiencies incurred by the composite optimization step, as the free-size result predicts only 103kN failure load.

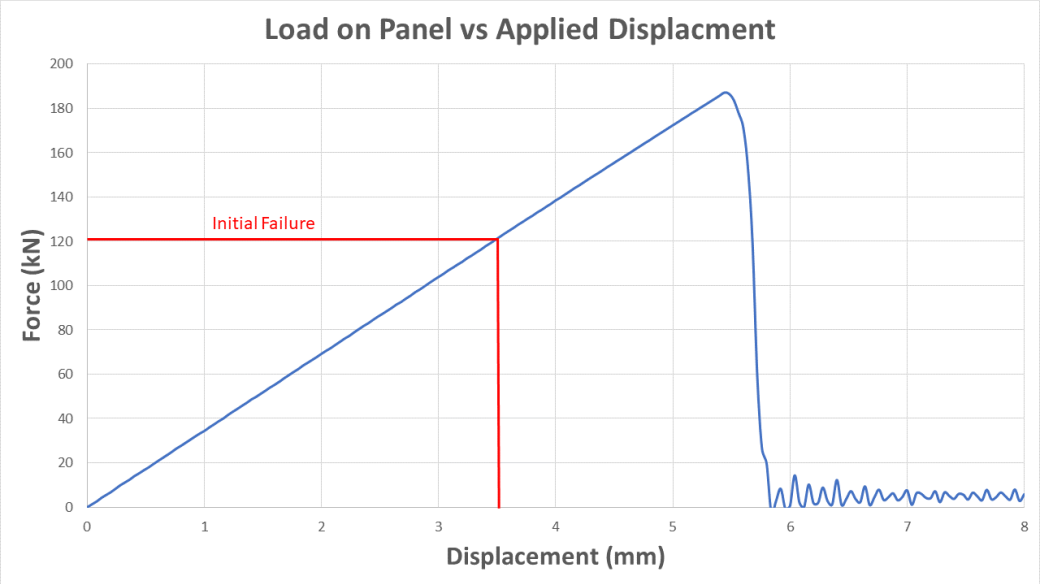

Figure 4.12: Evolution of load on the panel, as a function of applied displacement with out-of-plane nodal motion restricted.

In contrast, the explicit simulation carried out using Hashin criteria allows analysis past the initial failure condition. While the initial failure load predicted by the Hashin failure criteria is 121kN, Fig. 4.12 shows an essentially unchanged linear stiffness, with $34.6\frac{kN}{mm}$ before failure, and 34.0 $\frac{kN}{mm}$ afterward until ultimate failure. This ultimate failure occurs at a peak load of 187kN.

Criteria	Failure Load
Design	100kN
Tsai-Wu (Free Size)	103kN
Tsai-Wu (Composite Size)	112kN
Hashin (Initial)	121kN
Hashin (Ultimate)	187kN

Table 4.1: Critical loads and their relevancy.

The discrepancy between Tsai-Wu and Hashin (initial) failures may be attributed to multiple factors. First, they are simply different approaches to predicting failure, and so different ultimate loads would be expected [17]. Second, there may be unforeseen consequences of constraining the panel to eliminate the buckling mode. The buckling mode was suppressed by restricting all nodes' out-of-plane motion. Finally, the explicit simulation run using Hashin criteria incorporates strain hardening and energy dissipation aspects not present in the simpler Tsai-Wu simulation.

Despite these discrepancies between simulations, the ultimate failure mode predicted by the Hashin criteria qualitatively reflects JAXA's demonstration panel. The compressive and tensile cracks in the fiber predicted in 4.13 are present in 4.14.

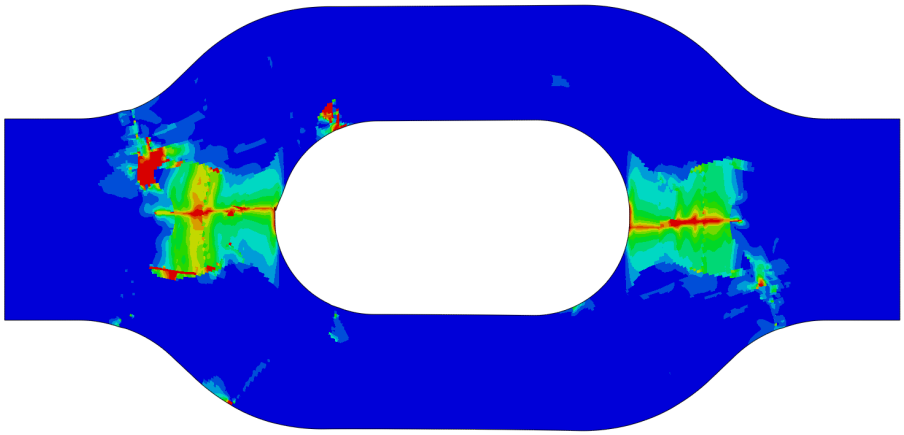

(a) Simulation of panel showing fiber compressive failure.

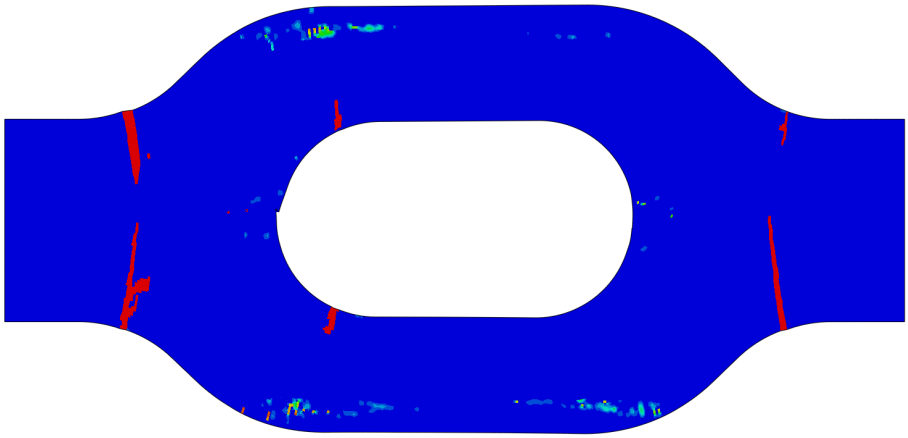

(b) Simulation of panel showing fiber tensile failure.

Figure 4.13: Illustration of ultimate material failure, as evaluated using an explicit FEA simulation, and Hashin failure criteria.

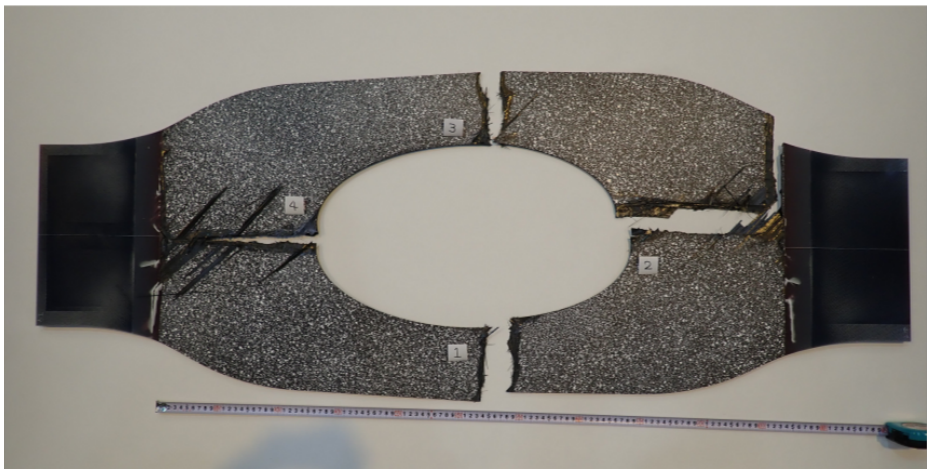

Figure 4.14: JAXA's panel after destructive tensile testing, shows a failure mode similar to that predicted via FEM. [15]

Chapter 5

MANUFACTURING DEMONSTRATION

Validation of this technology requires a demonstration part produced on an AFP system, such as the Electroimpact AFP robot at the University of Washington's Advanced Composites Center. The following outlines the steps required to create a part program, and how the additional tow-optimization allows this manufacturing to function.

The software used to generate machine-readable M and G code for Electroimpact AFP machines is "Vericut Composite Programming" or VCP. VCP does not operate using finite elements, rather using surface models to generate machine paths, and so the finite element model must be transformed. A pre-built tool in Hyperworks is available, with user-configurable parameters defining the boundary smoothing applied during the transition. Ranging from an element level recreation of the surface, to a smooth contour. Other brands of AFP equipment may use VCP, or other products e.g. CATFiber, which operate in a similar manner.

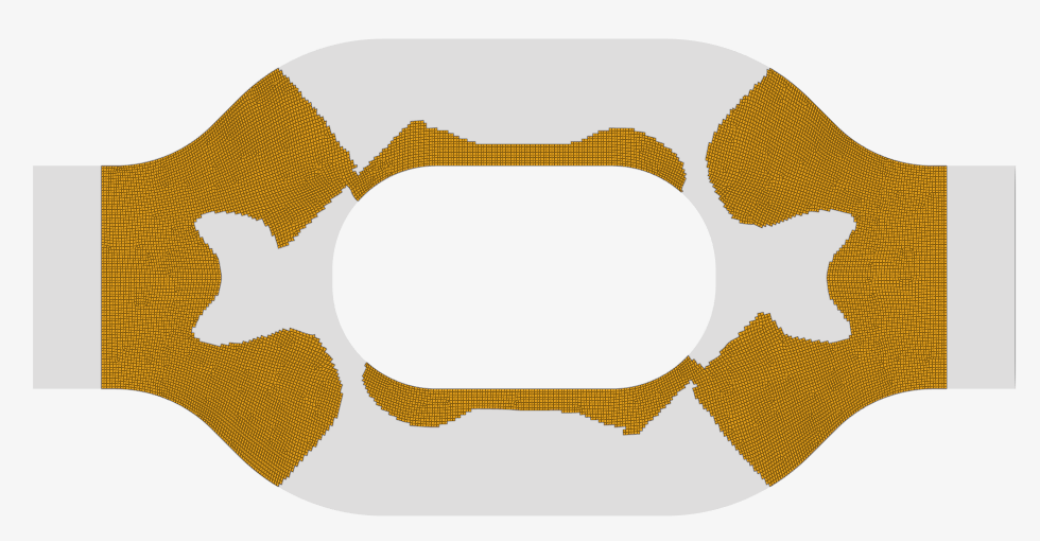

(a) Elements comprising an optimized ply.

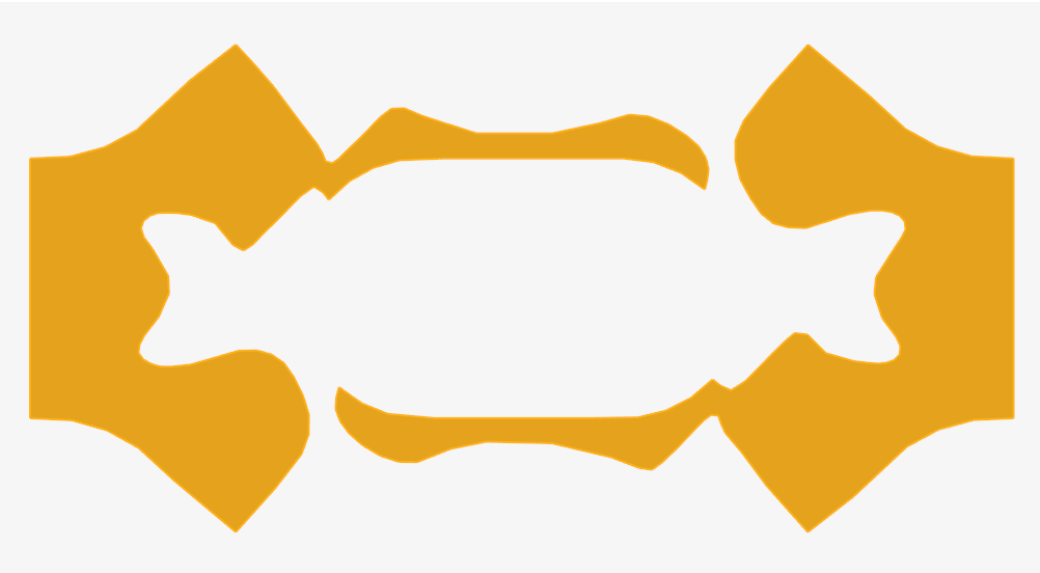

(b) Smoothed ply boundaries as a surface.

Figure 5.1: Ply surface generated from finite elements.

Then, this surface must be imported into VCP where individual courses are generated, and tow adds and cuts are specified. It is here where ply boundaries under the minimum tow length must be accommodated, manually specifying excess tow length be placed outside the boundaries of the finished part perimeter, rather than inside. Off-part motion is also specified, controlling the order courses are deposited, as well as ensuring the head does not intersect tool geometry.

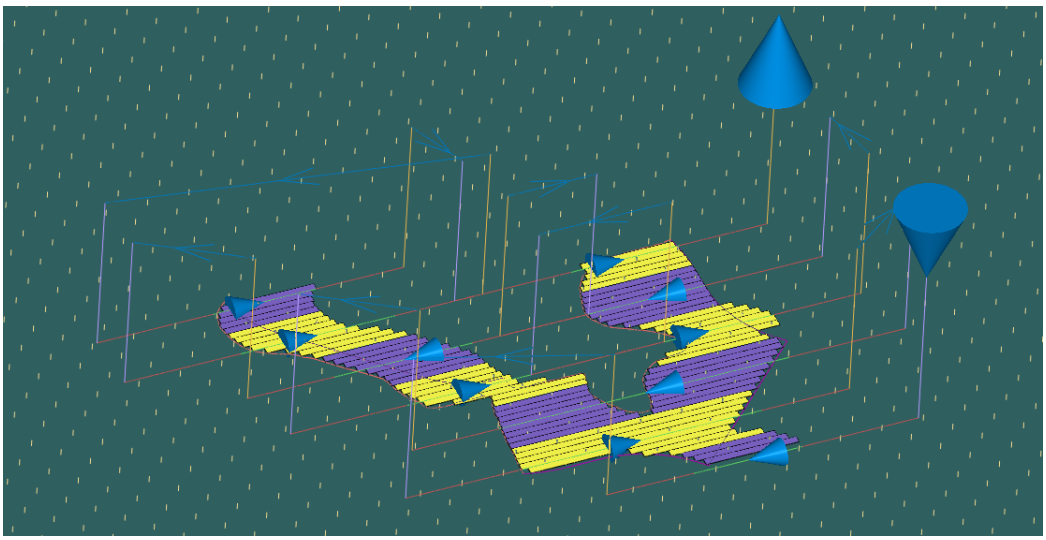

Figure 5.2: Single ply with courses, tows, and off-part motion shown.

Note here the flexibility in the tow generation. Unlike the solution proposed by Altair's current implementation, tows are not required to start at any particular point relative to the edge of the design space. Further, they are not required to start at the same point as their neighbors, or have a length equal to a multiple of the minimum length.

Finally, a machine specific post-processor is used to export these tow paths and machine motion as M and G code, and the panel can be created. After manufacture, tensile testing of the finished part may validate the optimization and analysis processes.

Chapter 6

CONCLUSION

While AFP is a powerful technology for the manufacture of large scale composite structures, it presents unique constraints which designers must be mindful of. Computational tools are becoming an essential part of the design process, and as more design work is outsourced to these algorithms they must also incorporate these constraints in order to remain effective. The success of this project is demonstrated by the delivery of the following:

- A method by which a design constraint for minimum tow lengths could be structured. This method of ply-modification is described herein, in such detail as to be reproducible. A patent application has been filed on this method.

- Code to implement this constraint. This code is available on request, and was essential in demonstrating the ply-modification method. Its current quality is satisfactory for academic work, and future upgrades will allow for commercial use.

- Demonstration of optimization process with and without constraint applied. This was demonstrated both for the process-demonstrator panel, as well as the alternative geometries and loading conditions outlined in appendices. VCP programming shows improved adherence to ply boundary capabilities of an AFP machine.

- Analysis of results. Detailed simulations of the test panel were carried out in Abaqus, and their results compared to real-world experiments from JAXA. The results of these simulations resemble the experiment both in their ultimate failure locations, as well as the unexpected appearance of a buckling failure mode.

6.1 Future Work

This process can be expanded upon. For example, the minimum threshold for discarding a tow is adjusted to reach the minimum mass. Currently, this is approached via a simple bisection search:

Initially, plies of any length below the minimum are discarded, and peak Tsai-Wu criteria evaluated. This will almost certainly result in a panel failure due to the large quantity of removed material, so the discard threshold is then increased to $\frac{1}{2}$ of the minimum tow length, and the process repeated. If this new analysis shows the panel passes, then the threshold can be reduced to $\frac{1}{4}$ of the minimum, or if it fails, increased to $\frac{3}{4}$. This search continues until the peak failure criteria is within some ϵ of 1.

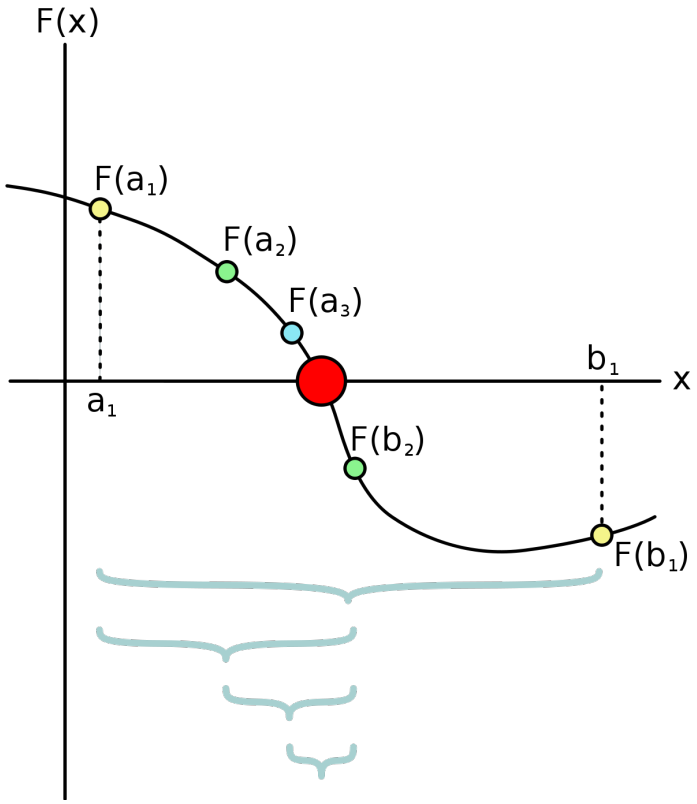

Figure 6.1: Illustration of bisection method to find a minimum. [18]

This process could be further refined by applying separate thresholds for each ply, or even tow-by-tow. However, this would dramatically increase computational costs and would require a carefully considered implementation. Additionally, results from the stress analysis could be fed back into the tow-removal algorithm. Perhaps prioritizing the preservation of very short tows, if they are in high-stress regions would result in an even more optimized structure, while maintaining manufacturability.

The overall design process could also be improved. Incorporating buckling constraints within the optimization process would result in an improved final product, but would require cooperation with the solver development team for implementation. Additional parameters should also be accounted for during the optimization process, such as inter-lamina shear stress around panel edges.

BIBLIOGRAPHY

[1] Quality Magazine, "How Laser Templating Tech Supports the Composites Industry." https://www.qualitymag.com/articles/96815-how-laser-templating-tech-supports-the-composites-industry, 2022. [Online; accessed 21-March-2022].

[2] Elevated Materials, "Carbon Fiber Weaves: What they are and why to use them." https://www.elevatedmaterials.com/carbon-fiber-weaves-what-they-are-and-why-to-use-them/, 2019. [Online; accessed 11-March-2022].

[3] T. Rudberg, J. Nielson, M. Henscheid, and J. Cemenska, "Improving AFP Cell Performance," *SAE International Journal of Aerospace*, vol. 7, pp. 317–321, 09 2014.

[4] Composites World, "The First Composite Fuselage Section for the First Composite Commercial jet." https://www.compositesworld.com/articles/the-first-composite-fuselage-section-for-the-first-composite-commercial-jet#carousele09e0d8d-9dc1-4ca6-bede-189622fdc133, 2018. [Online; accessed 11-March-2022].

[5] S. Ekşi and K. Genel, "Comparison of mechanical properties of unidirectional and woven carbon, glass and aramid fiber reinforced epoxy composites," *Acta Physica Polonica A*, vol. 132, pp. 879–882, 09 2017.

[6] A. G. M. Michell, "The limits of economy of material in frame-structures," *Philosophical Magazine Series 1*, vol. 8, pp. 589–597, 1904.

[7] K. Yamaguchi, S. Phenisee, Z. Chen, M. Salviato, and J. Yang, "Ply-drop design of non-conventional laminated composites using bayesian optimization," *Composites Part A Applied Science and Manufacturing*, vol. 139, p. 106136, 10 2020.

[8] W. Prager, "Nearly optimal design of trusses," *Computers & Structures*, vol. 8, no. 3, pp. 451–454, 1978.

[9] K. Suzuki, S. E. Phenisee, and M. Salviato, "An isogeometric framework for the modeling of curvilinear anisotropic media," *Composite Structures*, vol. 266, p. 113771, 2021.

[10] L. Esposito, A. Cutolo, M. Barile, L. Lecce, G. Mensitieri, E. Sacco, and M. Fraldi, "Topology optimization-guided stiffening of composites realized through automated fiber placement," *Composites Part B: Engineering*, vol. 164, pp. 309–323, 2019.

[11] C. Luo and J. K. Guest, "Optimizing topology and fiber orientations with minimum length scale control in laminated composites," *Journal of Mechanical Design*, vol. 143, 09 2020.

[12] Altair, "Analysis Origins: Optistruct." https://www.altair.com/newsroom/articles/analysis-origins-optistruct, 2019. [Online; accessed 13-March-2022].

[13] Altair, "Optistruct User Guide." https://2020.help.altair.com/2020.1/hwsolvers/os/topics/solvers/os/user_guide_os_c.htm, 2022. [Online; accessed 30-September-2021].

[14] Altair University Team, *Introduction to Practical Aspects of Composites with Altair OptiStruct*. 1820 E. Big Beaver, Troy, Michigan, USA: Altair, 2021.

[15] Y. Aoki, S. Sugimoto, Y. Iwahori, and T. Nakamura, "Manufacturing and evaluation of an optimized composite panel with a cut-out," *33rd Technical Conference of the American Society for Composites 2018*, pp. 1350–1357, Jan. 2018. 33rd Technical Conference of the American Society for Composites 2018 ; Conference date: 24-09-2018 Through 27-09-2018.

[16] T. Kremer and H. Schürmann, "Buckling of tension-loaded thin-walled composite plates with cut-outs," *Composites Science and Technology*, vol. 68, no. 1, pp. 90–97, 2008.

[17] C. Sun, J. T. B.J. Quinn, and D. Oplinger, "Comparative Evaluation of Failure Analysis Methods for Composite Laminates.," tech. rep., Purdue University, School of Aeronautics and Astronautics, May 1996.

[18] Wikipedia contributors, "Bisection method — Wikipedia, the free encyclopedia." https://en.wikipedia.org/w/index.php?title=Bisection_method&oldid=1076584140, 2022. [Online; accessed 25-March-2022].

Appendix A

VERTICAL LOADING ALTERNATE GEOMETRY

To illustrate the broad capabilities of my development, I have prepared some alternative examples of loading conditions optimized via Optistruct. The following setups are taken from "Topology optimization-guided stiffening of composites realized through Automated Fiber Placement" [10].

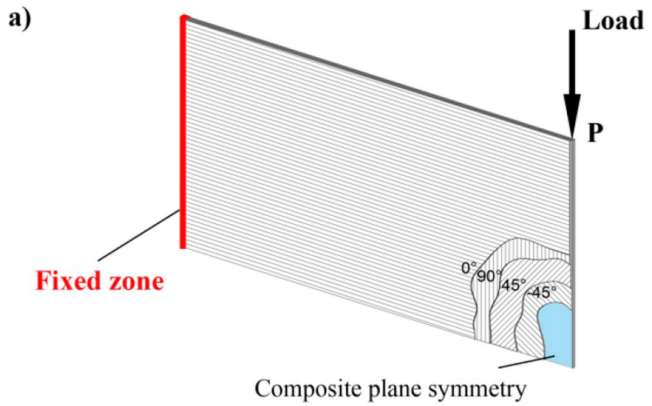

Figure A.1: Illustration of alternate loading condition from [10].

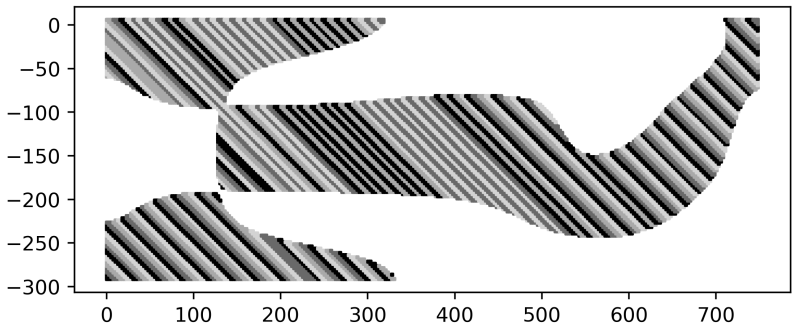

(a) Sample ply before AFP-compatibility.

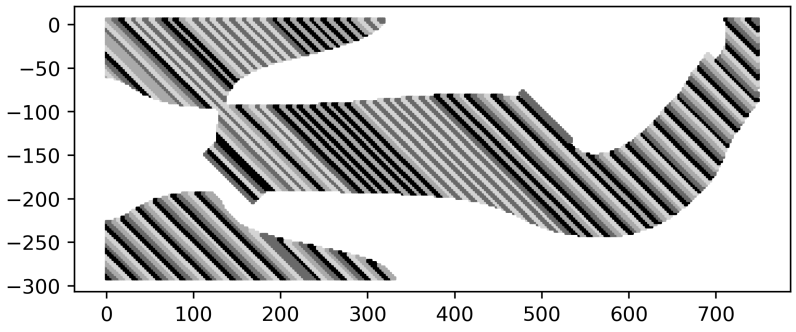

(b) Sample ply after AFP-compatibility.

Figure A.2: Illustration of process in alternative geometry.

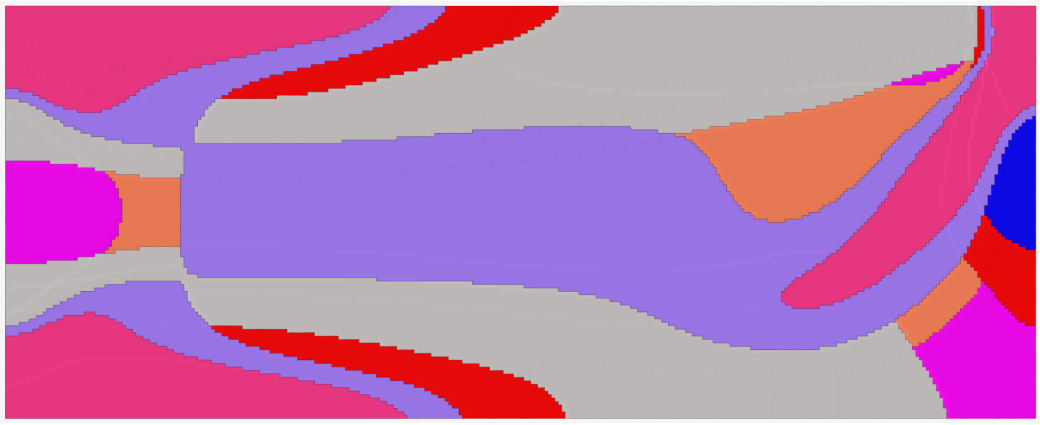

(a) Laminate before AFP-compatibility.

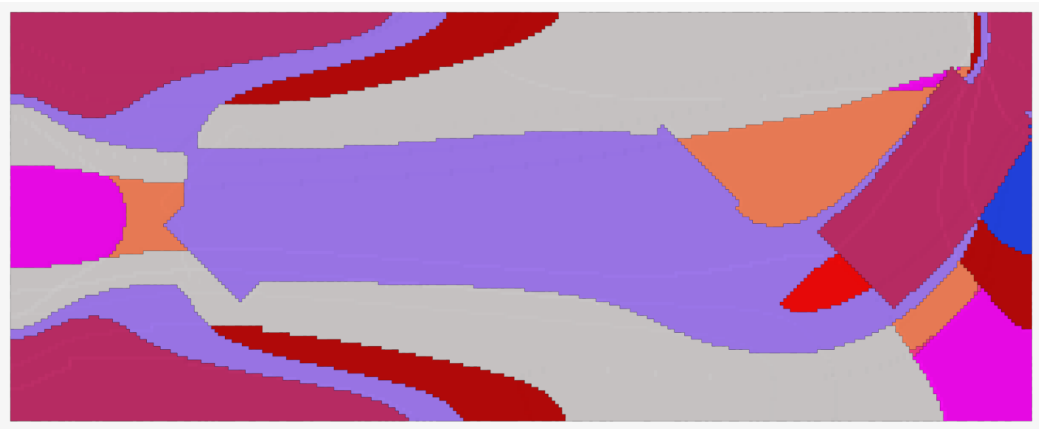

(b) Laminate after AFP-compatibility.

Figure A.3: Ply-stack before and after compatibility. Plies shown by colors.

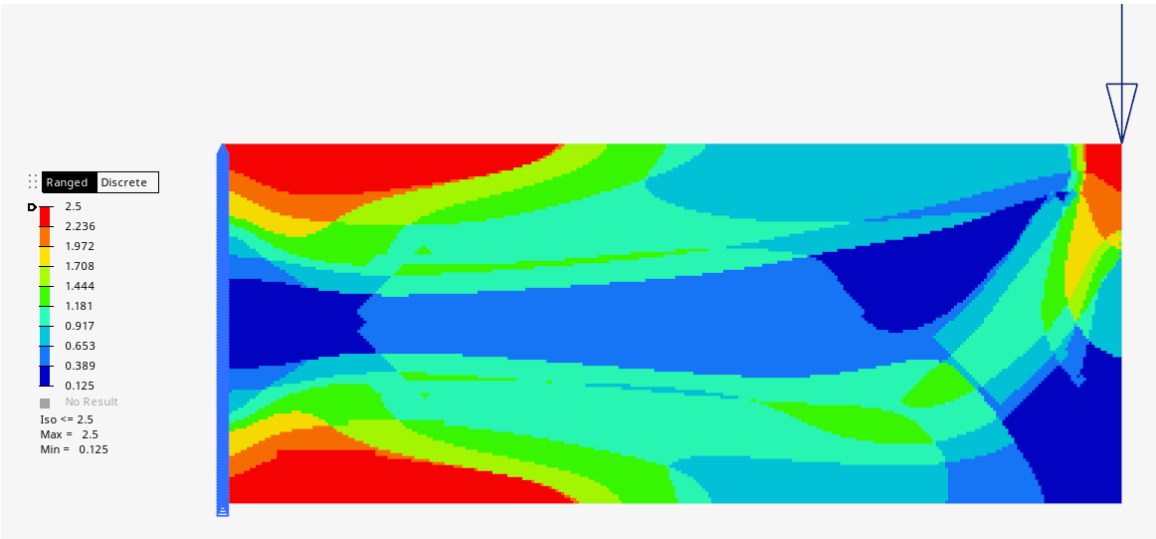

Figure A.4: Thickness of optimized panel. (mm)

Appendix B

MOMENT LOADING ALTERNATE GEOMETRY

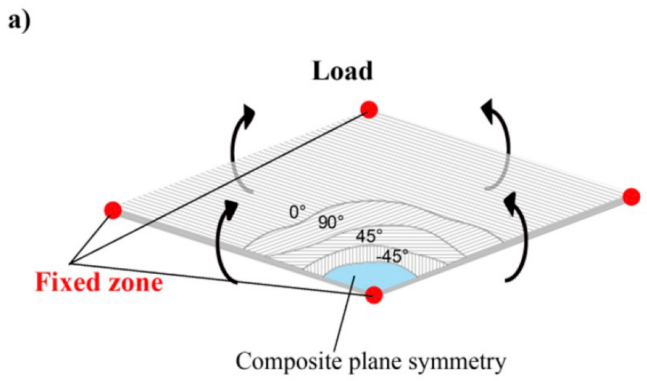

Figure B.1: Illustration of alternate loading condition from [10].

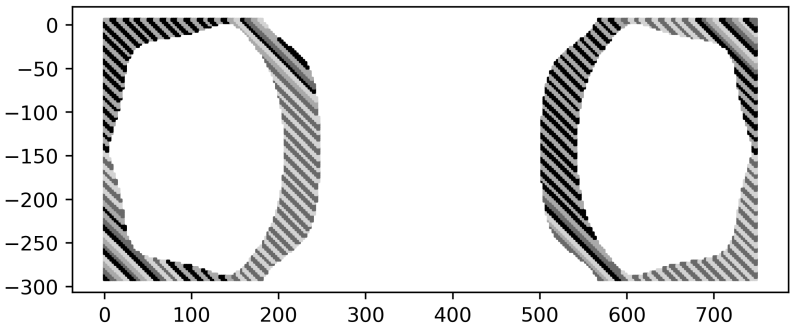

(a) Sample ply before AFP-compatibility.

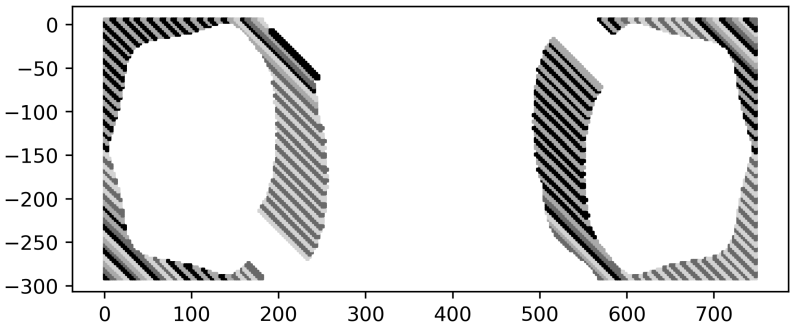

(b) Sample ply after AFP-compatibility.

Figure B.2: Illustration of process in alternative geometry.

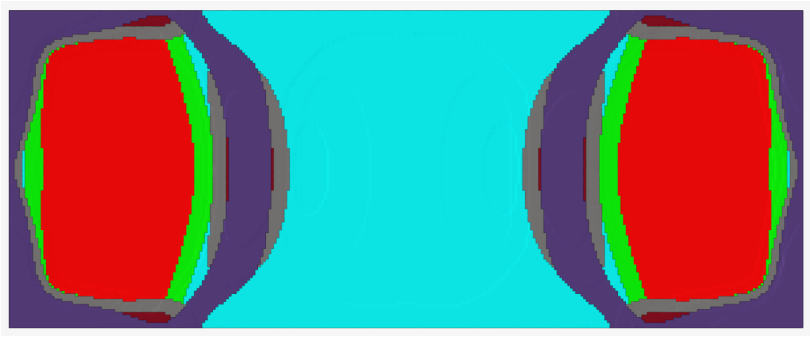

(a) Laminate before AFP-compatibility.

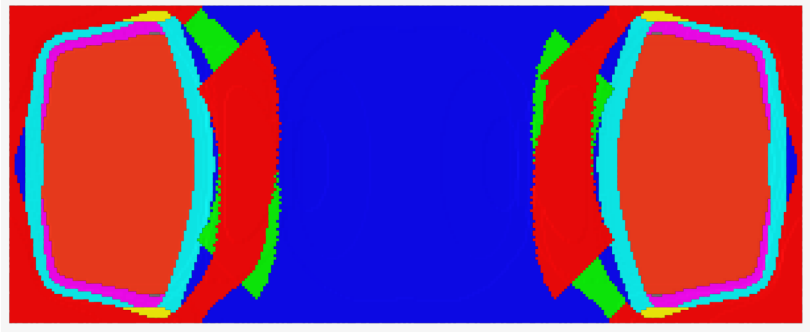

(b) Laminate after AFP-compatibility.

Figure B.3: Ply-stack before and after compatibility. Plies shown by colors.

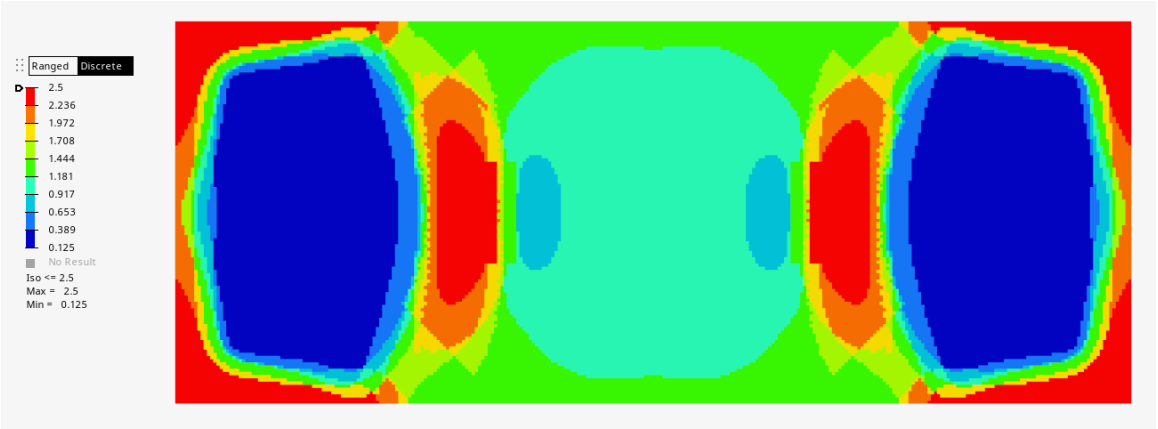

Figure B.4: Thickness of optimized panel. (mm)

Appendix C

OUT OF PLANE LOADING ALTERNATE GEOMETRY

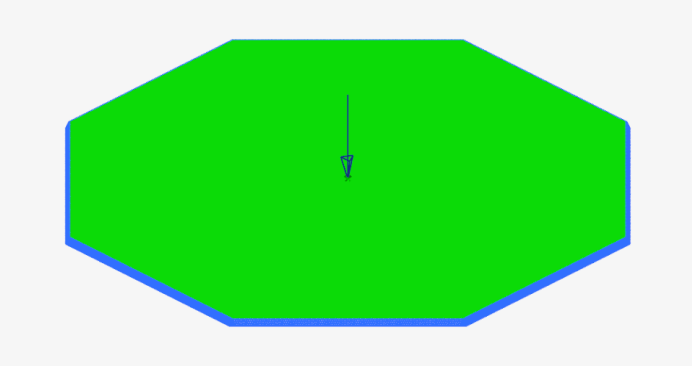

Figure C.1: Illustration of out-of-plane loading condition.

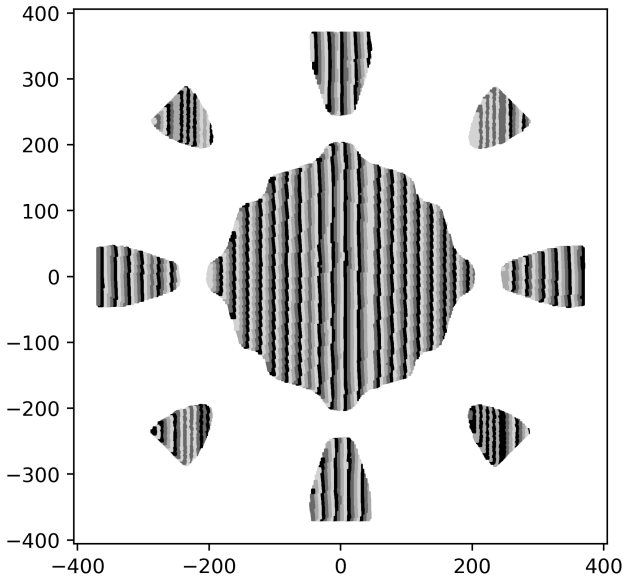

(a) Sample ply before AFP-compatibility.

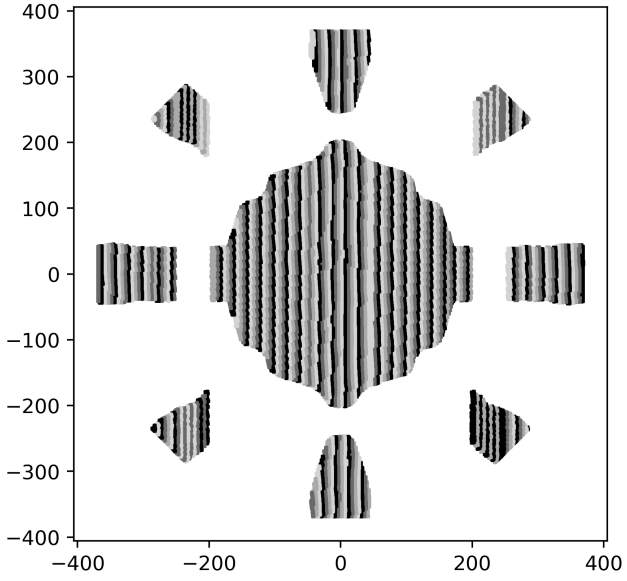

(b) Sample ply after AFP-compatibility.

Figure C.2: Illustration of process in alternative geometry.

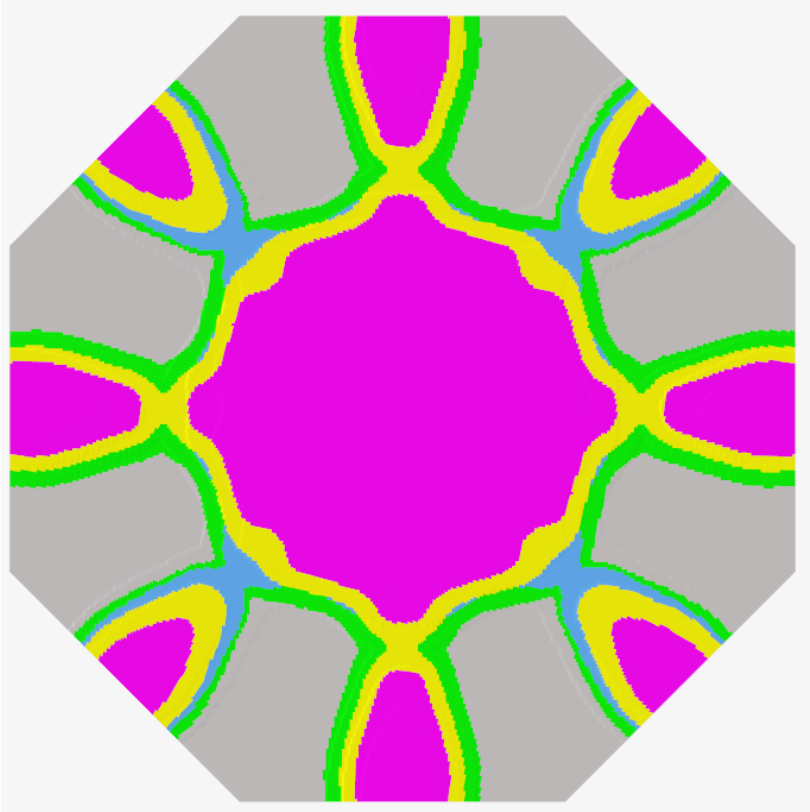

(a) Laminate before AFP-compatibility.

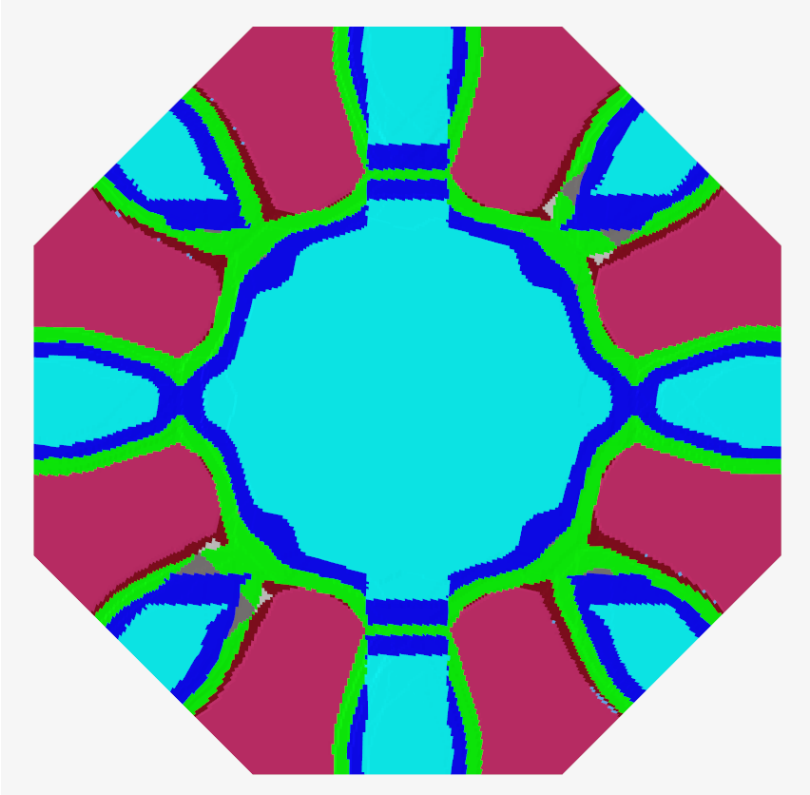

(b) Laminate after AFP-compatibility.

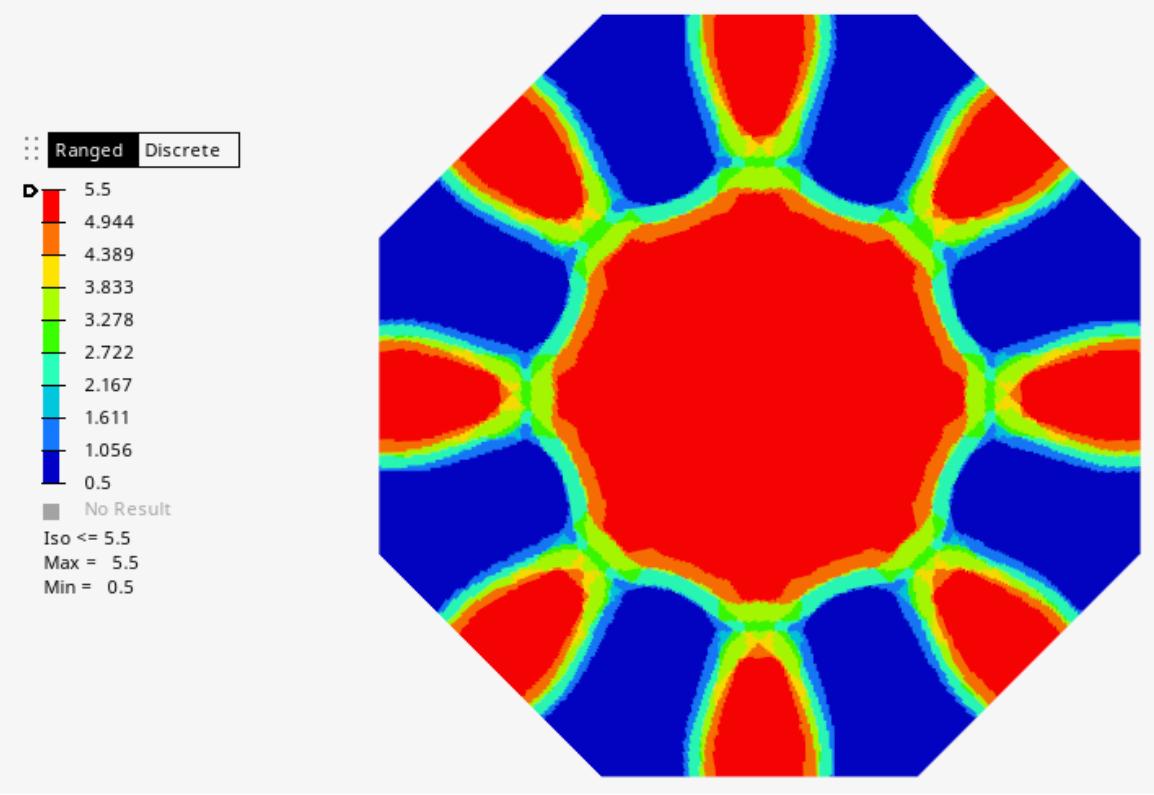

Figure C.4: Thickness of optimized panel. (mm)